A New Method For Fabrication of Medical Microfluidic Devices

By

Shiva Dahar
4323971

Thesis for the degree of

Master of Science

in Biomedical Engineering, Biomedical Electronics

Delft University of Technology

Supervisor:	Prof. dr. R. Dekker
Committee:	Prof. dr. R. Dekker Prof. dr. P.J. French Dr. G. Pandraud

August 2016

TU Delft

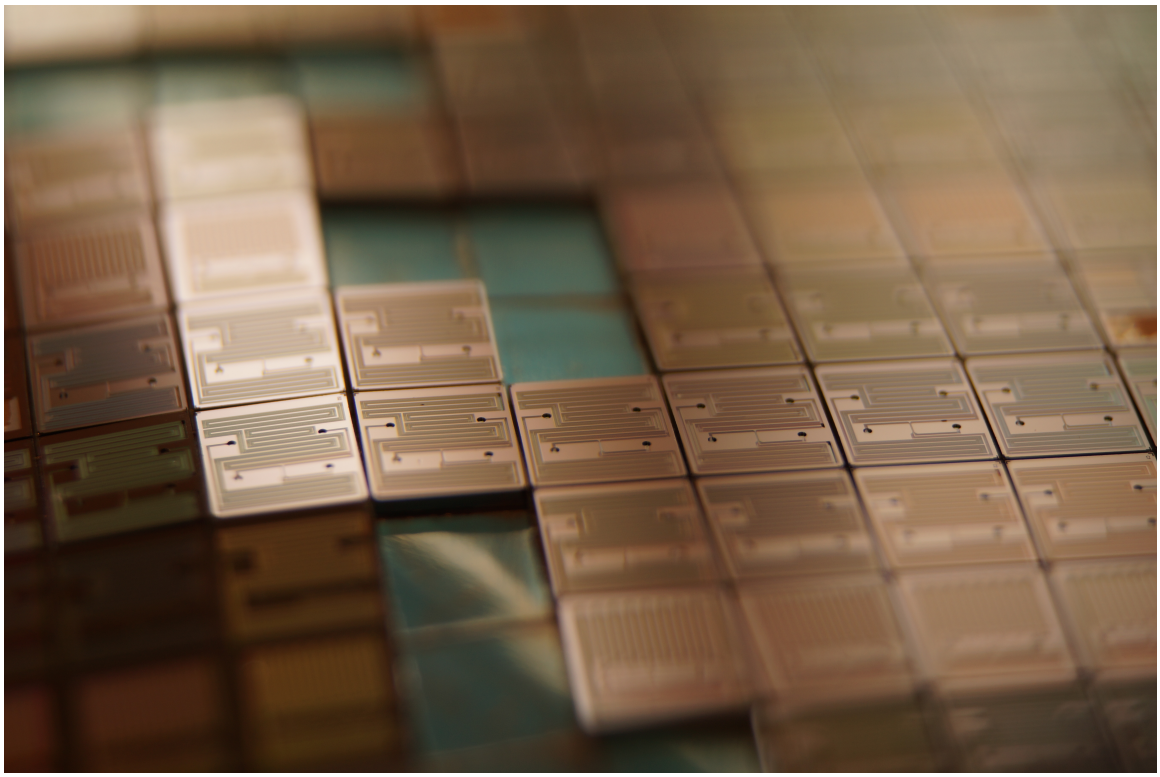

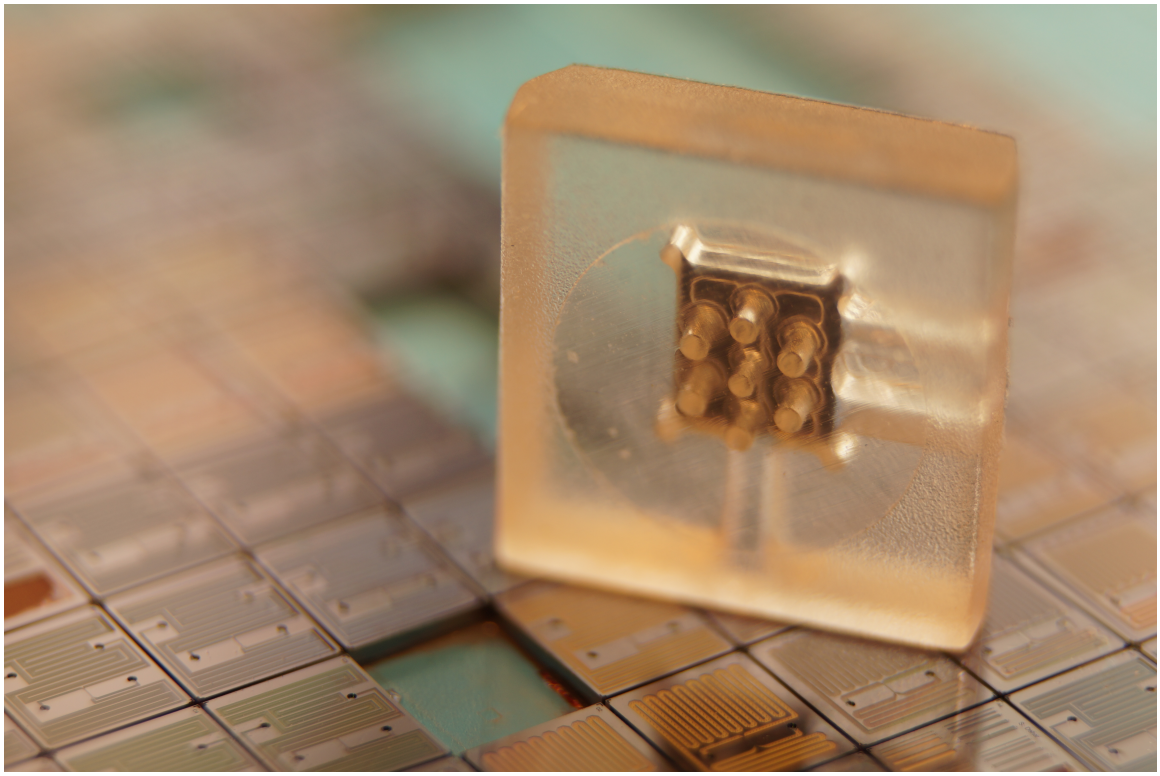

Abstract

This thesis presents a fabrication process for medical microfluidic devices that is performed with purely silicon microfabrication methods, which is a better option for mass-production than commonly used soft lithography. The fluids passing through the channels of a microfluidic device that is fabricated using this developed method can be observed through a thin layer of silicon dioxide and thus solving the problem of silicon being opaque to light. The new method also allows for addition of electronic sensors to the fabrication of the microfluidic devices.

Using the developed microfabrication method mentioned above, a medical microfluidic device working with cell mechanobiology principles to test and develop medicine is designed and presented. The device first measures the transit time of a cell passing through a restriction section with a width smaller than the cell diameter. The cell then passes through a long serpentine channel where it is treated by a medicine that is under development. The medicine diffuses into the microchannels with diseased cells from another microchannel that is running parallel with the cell channels through a porous membrane. The cells pass through another restriction section after being treated and the transit time is measured again. Comparison of transit times before and after treatment is an indication of the effectiveness of the medicine being tested.

Table of Contents

1 Introduction

In medical studies and specifically drug testing, using microfluidics instead of larger sample sizes offers many advantages e.g. faster and cheaper experiments and homogeneous samples. However, the number of microfluidic devices currently in use in medical studies does not seem to reflect this [1, 6]. The main reason that has been preventing microfluidic devices from mass-production is the main material with which microfluidic devices are currently being manufactured: PDMS (Polydimethylsiloxane).

1-1 Microfluidic Devices

The term "Microfluidics" can be defined as the science technology of designing and manufacturing devices that can manipulate very small amounts of fluids in micro-channels that have at least one dimension smaller than 1 mm [1]. Microfluidic devices use very small amounts of samples for each analysis, and can provide results in a very short time. One of the first applications of microfluidic devices in medical studies included blood rheology. Today there are more applications of microfluidics in various fields. For example drug development, synthesis and delivery in the medical fields [2].

One of the parents of microfluidics field is microelectronics. The first significant progress in the microfluidic devices was in the 1980s, and it was due to progress in silicon microfabrication. However, the attempts of directly applying silicon microelectronics and microelectromechanical systems (MEMS) fabrication methods were soon discarded due to various reasons, and instead of silicon and glass, plastics –specially PDMS- soon became the main material used in fabrication of microfluidic devices [1, 2].

Originally, silicon and glass were materials of choice for manufacture of microfluidic devices, but the focus soon shifted on polymer substrates and in particular, PDMS. Various problems with silicon contributed to silicon being discarded after a few initial attempts in 1980s, including it being opaque to visible and ultraviolet lights, higher price and non-permeable to gasses. Silicon is also not very elastic, and thus not suitable for the manufacturing of active microstructures such as valves and pumps [1, 9]. However, pumps are usually in a separate device so low elasticity is not a significant problem. Ahn et al. (2007) attributes the success of PDMS and other polyimides to biochemical reliability, compatibility and ease of fabrication. PDMS is a suitable material for fabricating microfluidic devices during research, but it is not an industrial-friendly polymer. Companies prefer to use industrial polymers that are more cost effective and accessible and also easier to manufacture, but these polymers are not suitable for microfluidic devices [6, 9, 10]. If the main obstacle,

i.e. silicon being opaque to light is overcome, silicon is a much better option for mass production that can allow microfluidics to have a more wide spread use.

1-1-1 Advantages of microfluidic devices

There are several advantages for using a micro-analysis device in medical studies, Some of these advantages include:

1- Many chemicals and reagents used in studies can be very expensive and using them in microscales rather than macroscales allows for more experiments with lower costs [3].

2- Using large samples of biological material, results in a large variety in the test subject. For example in a specific disease, different cells can be in different stages of illness so their reaction to the test medicine will be different. What we see will be an average of different responses and may not be specific enough. However, micro-devices allow for cells to be chosen individually and the results can be attributed to a cell with a specific stage of disease [3, 5]. In the words of Yin et al. (2012): “An average of 50% protein expression in a cell population can represent either a 100% response in half the cells or a 50% response in all.”

3- Studying the effects of medicine involves diffusion of chemicals and biological reagents. This diffusion is much faster in micro-scales in comparison to macro-scales as the reaction probability of diffusion is higher in micro-scale. Practically, reaction times of microfluids are in ranges of seconds and minutes whereas experiments on large samples can take up to days [5].

4- Smaller samples naturally result in smaller amounts of harmful products [5].

5- Several consecutive tests can be added to one microfluidic device, in effect simulating a full barrage of tests that in macro-scales may even have to be performed in different laboratories [5].

1-1-2 Disadvantages of microfluidic devices

Microfluidics offer a lot of promises and advantages. However, the number of products in use does not seem to reflect this. Microfluidics are still in limited use. Any device that has been ever designed comes with both advantages and disadvantages. Microfluidic devices are not an exception to this rule. The disadvantages of these devices may be what has been

preventing their more wide spread use. Volpatti et al. (2014) mentions disadvantages that may have hindered commercial success of microfluidic devices.

Disadvantages of microfluidic devices include:

1- A Lack of standardization in designing microfluidic instruments. As a result, users may have difficulties connecting the device with other hardware, such as external pumps and pneumatic fluid handling systems [6].

2- Handling microfluidic devices may need additional training that is significantly different from more typical laboratory medical equipment that use larger samples [6].

3- As microfluidic devices work with miniscule samples, they have lower throughputs than equipment that work in macro scales. This characteristic may not always be a problem, but in some types of microfluidic systems such as droplet-based systems, low throughput is a disadvantage. Droplet based systems are mainly used for drug delivery and a low throughput results in low amounts of delivered medicine [4].

There is another reason that a microfluidic device may not be used in some experiments. This problem is not due to a disadvantage of the device, but related to the nature of the experiment itself. For example if there is a need for a sample preparation step before microfluidic tests, and this step will lower the speed of experiments on the device, then the device will not be used with its maximum efficiency and customers may find the device unnecessary [6].

As a result of the disadvantages mentioned above, users may not be willing to change their conventional practices and instruments. People are typically not very eager to change their conventional method of doing something if it works, unless the advantages offered by a new method are so great that they overcome the needed effort that must be put into using a new instrument. This great advantage is usually either a significant operational advantage or lower cost.

There are two main issues that if solved, can bring microfluidic devices closer to commercial use: Standardization and integration [6].

Standardization:

Unfortunately, currently there is a lack of proper standardization in the field of microfluidics. Researches in this field do not always report chip-to-chip variations in their new designs and reproducibility statistics. As a result, these new microfluidic instruments are not always compatible with previously existing associated devices (such as pumps). One of the biggest incompatibilities comes in the form of the dominant material used in fabricating microfluidic instruments: Polydimethylsiloxane, more commonly known as PDMS [9]. However, PDMS is an expensive polymer that is difficult to manufacture and scale up and thus not very suitable for mass-production. As a result, industrial companies are not willing to use PDMS as their main material. Companies prefer to use industrial polymers that are more cost

effective and accessible and also easier to manufacture and shape such as PMMA and polycarbonate. However, a device designed by academic researches in labs and manufactured with PDMS cannot be manufactured with other polymers due to differences in the characteristics of PDMS versus industrial polymers. Therefore researchers must find a new manufacturing method that is more compatible with industry [6, 10]. If the main disadvantage of silicon (i.e. being opaque to light) is overcome, it can be a suitable substitute for PDMS, as silicon chips are easy to mass-produce.

Integration:

Academic researches usually focus on the design of each individual microfluidic device, without much consideration of whether they are compatible with each other or with other existing devices. This integration problem follows the issue of a lack of standardization. For example, a lab-on-a-chip device consists of several components including pumps, voltage supplies and software. For an integrated microfluidic medical device to be successful, analysis should be able to seamlessly move from one step to the next. Another requirement for the success of a device is that there should be no need for prior preparation of the samples. A microfluidic device also should be operable by customers who are not microfluidic experts. [6]

Using silicon to fabricate microfluidic devices, can be a step toward solving the problem of standardization. Deciding on specific design parameters for PDMS microfluidic devices is very difficult as they are typically hand-made by individuals for research purposes. It is easier for factories doing silicon microfabrication to decide on specific parameters such as the placement and dimensions of inlets and outlets of various microfluidic devices, so they can all be connected to the same pumping system.

1-2 Cell Mechanobiology

Mechanobiology is a field of science that concentrates on the relation between changes in cell structure and tissue mechanics, and cell development, functions and diseases. Cells can be affected by mechanical stimulations. Mechanical stimuli directly influence cell functions such as cell contraction, differentiation and division. The cells translate these stimuli into biological signals by changing their Cytoskeletal structure and thus function. Cell mechanobiology performs analysis of cell mechanical properties in order to understand how cells sense the biomechanical stimuli and respond to them. Furthermore, many diseases such as cancer, malaria, inflammation and cardiovascular disorders can change mechanical properties of affected cells in comparison to healthy cells. [11, 12]

Microfluidic devices can be designed to measure mechanical properties of cells. Diseased cells can be compared with healthy cells. Also the effects of medicine can be observed by the

changes in mechanical properties of the cells [11, 12]. Figure 1 depicts how stimuli from the environment affect the cell mechanical properties through changing cytoskeletal structures, and that a disease can change how cytoskeleton responds to stimuli from the environment.

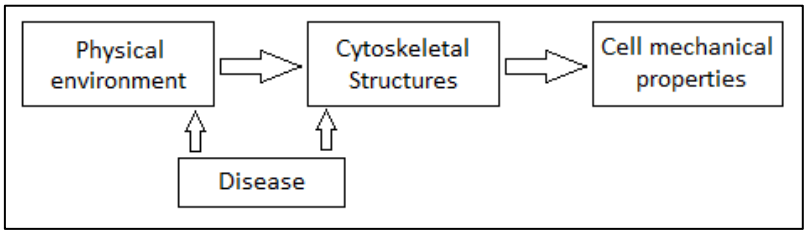

Figure 1: Stimuli from environment affect cell's mechanical properties through cytoskeletal structure

Ravetto (2015) connects the physical environment to mechanical properties of the cell through cytoskeleton:

1- "Organization of the cytoskeleton is influenced by biomechanical stimuli and the cell's physical environment." [13]

2- "Concentration and molecular architecture of the cytoskeleton determine the deformability and the mechanical response of the cell." [13]

Ravetto (2015) performed a study on cells based on mechanobiology. Revetto's microfluidic device investigated the effects of drugs on monocytes. The device consisted of two channels one above the other that were separated by a PDMS membrane that contained small pores. The inlet and outlet of the bottom channel were connected to two constriction sections. The top channel contained drugs that could enter the bottom channel through the porous membrane and affect cells in the bottom channel. The cells entered the bottom channel through one restriction section, were affected by medicine in the channel and passed another restriction section in the end. Ravetto treated the cells in the serpentine channel with an agent that weakened the cytoskeleton and measured entry time, transit time, elongation and recovery time of cells in the outlet restriction channel and compared them with the same measurements taken in the inlet restriction channel to see the effects of the agent. Figure 2 [13] shows a cell entering the inlet restriction section in Ravetto's device.

Ravetto observed a difference in transit velocity (calculated from transit time) between the non-treated and treated cells. Higher transit velocity in treated cells indicated the effect of the agent on the cells (reduce in stiffness).

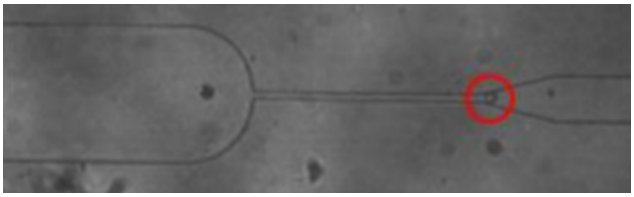

Figure 2: A cell (inside the red circle) entering the inlet restriction section in Ravetto's device. [13]

Later in this thesis, a novel microfluidic device is designed that uses cell mechanobiology to study the effects of medicine on cells in a way similar to Ravetto's device. In the new device that can be fabricated with silicon microfabrication methods, cells enter microchannels fabricated in silicon through an inlet and pass through a restriction area where their transit time is measured. The cells then travel through a serpentine channel where they have time to be treated by medicine then pass through another restriction section and their transit time is measured again. Change in change in transit time is an indication of effectiveness of the medicine.

1-3 Research Goal and Thesis Outline:

The aim of this research is to develop a fabrication method for microfluidic devices using purely silicon microfabrication techniques. A microfluidic device that uses cell mechanobiology principles to test the effect of medicine on cells is designed and fabricated with the new method. Such a device can be easily manufactured in the vast, already existing IC fabrication infrastructures. The fabrication method developed in this research can hopefully be a step towards mass-producible microfluidic devices. Using silicon microfabrication methods, also brings the possibility of adding various CMOS sensors to microfluidic devices.

In the thesis first in this chapter, microfluidic devices are defined and their advantages and also some of their problems are presented and then the concept of cell mechanobiology and its use in medical microfluidics are explained. In Chapter 2, an overview of the developed microfabrication process is presented. In Chapter 3, soft lithography (fabrication method used for PDMS) and silicon microfabrication are compared and examples of medical microfluidic devices in literature that are fabricated with silicon microfabrication methods are presented. Chapter 4 explains the design of the new microfluidic device and in Chapter 5, the fabrication is presented step by step. At last, conclusion of this research is presented alongside explanation on further work on this topic that has been performed by another student.

2 Microfluidic Device Fabrication Process Overview

In the previous chapters, the advantages of using microfluidic devices were explained. In this chapter an overview of the silicon microfabrication technique developed for fabrication of a microfluidic device (that works with mechanobiology principles) is presented. The design of the device is explained in Chapter 4 and the details of fabrication in Chapter 5.

2-1 Developing A Silicon Microfabrication Method For Microfluidic Devices

In order to fabricate a medical microfluidic device using only silicon microfabrication techniques, the main objectives are:

- Fabrication of microchannels *inside* silicon, which are only accessible from specific areas that act as inlets and outlets for microfluidics.

- All or at least parts of the microchannels must be transparent to light to allow for observation of cells that flow in the channels.

First a layer of silicon dioxide is deposited on the silicon wafer. Then in the areas where microhannels must be fabricated, small trenches are etched into SiO_2 and silicon very close to each other using deep reactive ion etching. Then the silicon sidewalls between these trenches are removed with isotropic etch, forming microchannels inside silicon while the dioxide layer on top of the channels remains. But this layer has holes in the shape of the original trenches that were etched in the silicon. These holes are now covered with deposition of another SiO_2 layer. Because the trenches have very small dimensions (a width of less than 1 μm), they are closed due to step coverage of silicon dioxide deposition. A thin layer of silicon dioxide is transparent to light, so the microfluids can be observed in the channels from above. A schematic of the steps of the developed fabrication method is presented in figure 3.

In the previous few attempts in fabricating microfluidic devices from silicon, microchannels were either etched in silicon in the form of grooves (Figure 5) and then covered with a glass plate to form channels or they were fabricated with etching through-holes (Figure 6) in a silicon wafer [14, 15]. This new fabrication method however does not require a separate glass plate to cover the channels. It also allows for fabrication of much smaller channels in comparison to microfluidic devices with through-holes. The developed microfabrication method has more advantages:

- Various features can be included in one single photomask to be fabricated at the same time; e.g. a wide range of microchannel sizes, inlets and outlets for microfluids accessible from the

top of the device, passive mixing structures (pillars in microchannels created with absence of a trench in the middle of a channel) and nozzles (big trenches in the middle of microchannels that are too big to be covered with SiO_2 layer deposition).

- After the channels have been covered, a flat silicon dioxide layer remains and the microfabrication can be continued with fabrication of sensors (e.g. thermal or optical sensors) on top of the channels that can provide automatic detection of cells.

The next section provides an overview of the fabrication steps of the developed process.

2-2 Fabrication Steps

Figure 3 shows a schematic of the overall fabrication process of micro-channels in a series of cross sections. Details for each step is explained in chapter 5. In Figure 3:

a: A bare 150 mm silicon wafer is used as substrate. A silicon dioxide layer is deposited with a thickness of 0.5 µm (dark blue layer in the picture). The wafer is coated with photoresist (yellow layer).

b: The photoresist is exposed in a stepper with a dark field mask. The mask has several designs for microfluidic channels in net like patterns with the exposed areas being rectangles and squares with various sizes (e.g. 0.6*2.4 µm) with a pitch of about 1.4 µm. The resist is then developed.

c: The exposed areas are dry etched. First SiO_2 layer is removed by etching with etch stop on silicon, then silicon is etched with DRIE method (timed etch for single-side polish wafers and etch stop on BOX in SOI[1] wafers). All the photoresist is lost in this step. Also, some of the SiO_2 layer is lost during Si DRIE.

d: Isotropic etching with CF_4 plasma is performed. The silicon under dioxide is etched while some of the dioxide layer is lost. If the silicon wall is thin enough that it is gone before the dioxide layer, the results is a hanging membrane with net-like structures made of SiO_2 over trenches etched in silicon. Figure 3-e shows a top view of this dioxide membrane. The red line shows where the cross sections are placed.

f: A new silicon dioxide layer is deposited on the wafer (light blue), closing the holes in the dioxide membrane. Now we have channels inside the wafer that have been covered from the top and are accessible only from specific positions that act as inlets and outlets for the micro-fluids.

[1] Solid on Insulator

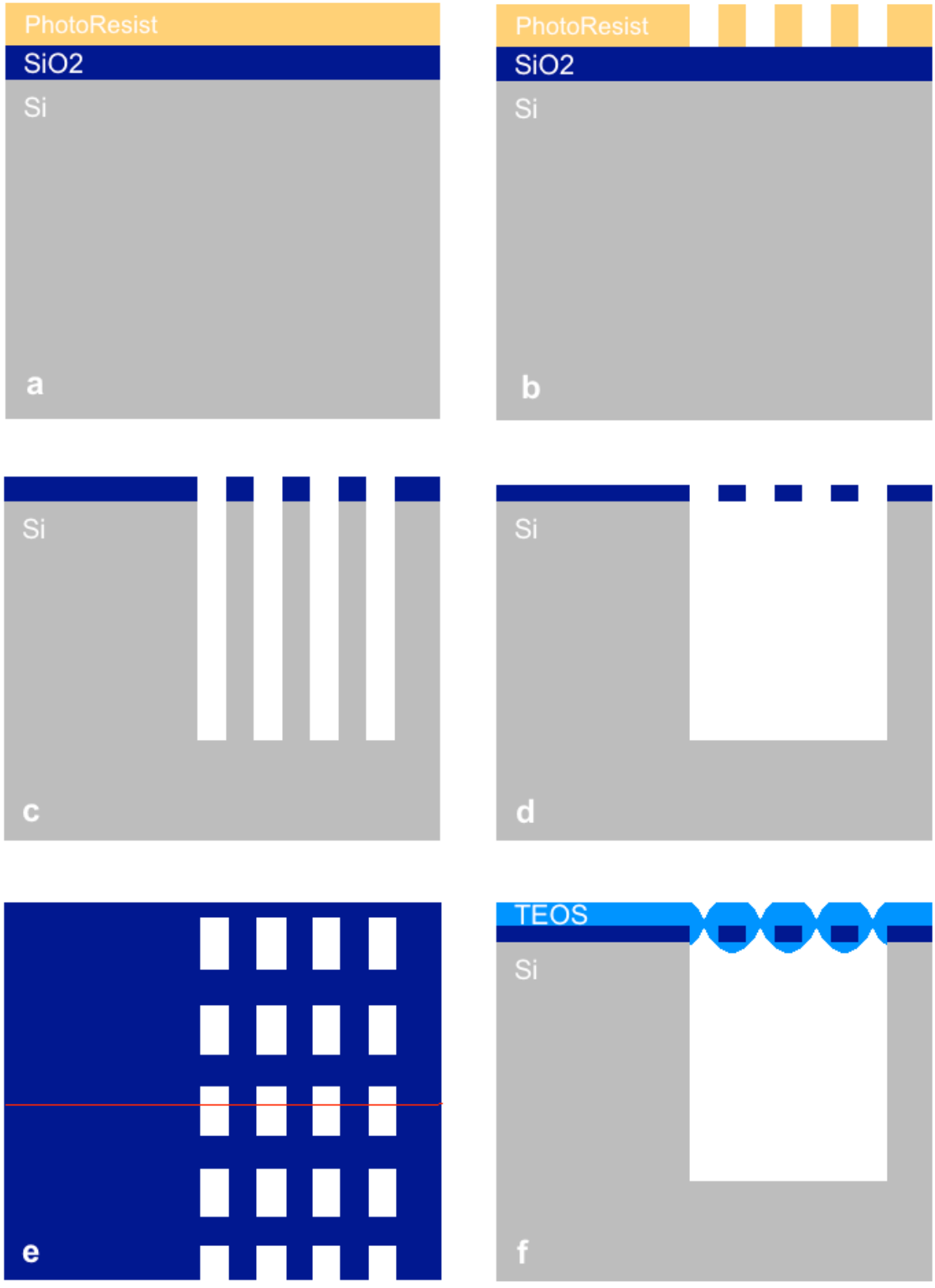

Figure 3: Microfluid channel fabrication steps (cross section view).

2-2-1 Fabrication Considerations

The fabrication method explained in the previous section, depends on exposure and DRIE of very small trenches and then removing the silicon sidewalls while keeping the dioxide membrane. All these steps have special requirements to be successful and sometimes these requirements clash and a tradeoff happens. These requirements must be considered during the design of the trenches.

Minimum trench size: The size of trenches limits the thickness of the photoresist layer used in lithography. If the photoresist is too thick, proper exposure will be a problem. In literature, resolutions achievable with various photoresists are investigated by exposing lines with different widths. However the features that were exposed in this research were in shape of rectangles and squares. A square with a side length of 1 μm is more difficult to expose than a line with a width of 1 μm. Because no literature was found on resolution and exposure parameters of several small rectangles or squares close to each other, a variation of trench sizes were included in the mask design to find the one most suitable.

In case of DRIE, smaller trench opening means slower (and thus longer) DRIE. Longer DRIE results in more loss of the masking layer (first photoresist and then SiO_2).

Maximum trench size: Trenches that are too wide, cannot be closed with step coverage of SiO_2 deposition.

Minimum trench distance: Trenches that are too close to each other may connect during lithography and create a bigger trench.

Maximum trench distance: Increasing the width of the sidewalls results in longer CF_4 etch. However CF_4 not only etches silicon but also SiO_2 just at a slower rate. Long CF_4 etch removes the SiO_2 membrane.

The table below shows the limitations put on trench design by various fabrication steps.

Fabrication steps / feature limits	Lithography	DRIE	CF_4 sidewall etch	Trench Closing
Trench width min.	X	X	-	-
Trench width max.	-	-	-	X
Trench distance min.	X	-	-	-
Trench distance max.	-	-	X	-

Table 1: Fabrication steps put limitations on design. The top row holds the names of limiting steps and the left colomn holds the features on which the limitations are put. In the table, An “X” indicates the existance of a limitation.

2-3 Observation Area On SOI Wafers:

The microfluidic device fabricated in this research was designed to be compatible with a special plastic holder that could be connected to a pumping setup. The plastic holder covered the top of the microfluidic device and allowed for micro-needles to pass through openings in the holder and pump fluids through outlets and inlets of the device. As the microfluidic device was covered from the top, any needed observations had to be made from the bottom. The pumping setup allowed for observation of a specific area of the microfluidic device with microscope from the bottom, so that are had to be transparent to light. But silicon is opaque to light. This problem can be solved with using silicon on insulator (SOI) wafers.

The complete fabrication process of the microfluidic device requires silicon on insulator (SOI) wafers that can be worked on from both sides. SOI wafers have a buried oxide layer (BOX) close to the front side, while the backside is covered with SiO_2. The SOI wafers used for the microfluidic device in this research had a 1 µm thick layer of thermal SiO_2 buried 40 µm deep from the front side (top in Figure 4) and another 1 µm thick layer of thermal SiO_2 covered the back. In SOI wafers, DRIE of the surface stops on the BOX layer (Figure 4-a). Then after lithography on the back, the wafer is etched (DRIE) to allow for observation of specific parts of the channels from the back.

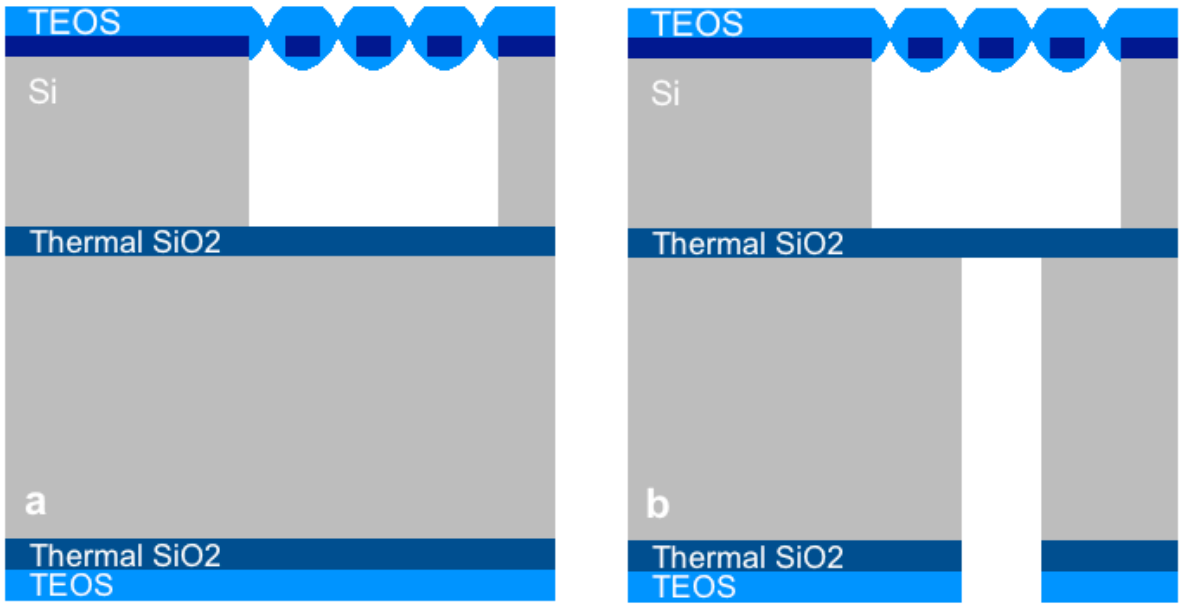

Figure 4: Microchannels on SOI wafers. **a)** Trenches etched in SOI wafers stop on BOX layer. The light blue SiO_2 layer on the back of the wafer is drawn because the trenches are covered with TEOS PECVD silicon dioxide which is deposited on both sides of the wafer. **b)** Backside etch.

3 Soft Lithography And Silicon Microfabrication

Originally, silicon and glass were materials of choice for manufacture of microfluidic devices, but the focus soon shifted on polymer substrates and in particular, polydimethylsiloxane (PDMS). There are several possible reasons as to why this switch from silicon to PDMS happened:

- Silicon is opaque to visible and ultraviolet lights. [1]

- Silicon is more expensive to use in academic research settings, as silicon microfabrication needs clean room facilities, while PDMS can be used in simpler facilities. [1, 3]

If the problem of silicon being opaque to light is solved, then investing more expenses and effort on silicon will be well worth it due to various advantages that silicon offers:

- Microelectronic and IC manufacturing methods can be used for mass-production of microfluidic devices in contrast with PDMS that is not an industrial polymer and unsuitable for mass production. [1, 6, 9, 10]

- Possibility of adding various detectors by combining their manufacturing steps with the microfluidic device, for instance thermal, pressure or optical sensors. [9]

- Silicon microfabrication allows for automated, and thus faster production.

Polymeric substrates such as PDMS are manufactured with a method called Soft Lithography, while silicon microfabrication reigns the world of IC fabrication. Most of the soft lithography steps can be done in simple chemical labs, however it still requires some silicon microfabrication techniques in the first few steps [13]. Silicon microfabrication, although more expensive during research, has the advantage of being fully automated in industries.

Basically, *PDMS is cheaper when used in research, while silicon will be less expensive in mass-production.*

3-1 Silicon Microfabrication And Microfluidic Devices

The main use of silicon microfabrication methods in fabrication of Microfluidic devices is for emulsion microchannels for droplet generation [14-16]. As mentioned previously, polymers and specially PDMS have replaced silicon as the main material for fabrication of medical microfluidic devices. However, PDMS is not an industrial polymer, which is part of the

reason these devices have not had much commercial success [10, 17]. Developing a process to apply current silicon microfabrication methods to microfluidic devices will be a great help in commercialization of microfluidic devices.

There are not many studies on microfluidic devices that purely use silicon microfabrication methods. The existing studies are mostly decades old. Kikuchi et al. (1992, 1994) and Kobayashi et al. (2002) are a few examples. In more recent years, there have been studies in which the designed devices are a hybrid of both soft lithography and silicon fabrication. However, these types of devices still suffer the problems that come with the necessity of using soft lithography.

Kikuchi et al. (1992) designed a simple microfluidic device using silicon microfabrication methods to observe behavior of blood cells. Kikuchi et al. etched microgrooves in a silicon substrate using photolithography. The substrate was then covered by glass, forming microchannels. Blood flowing through these channels allowed for microscopic observation of the cells. The grooves were etched using wet anisotropic etching on <100> silicon, resulting in 'V' shaped grooves as depicted in Figure 3. [14]

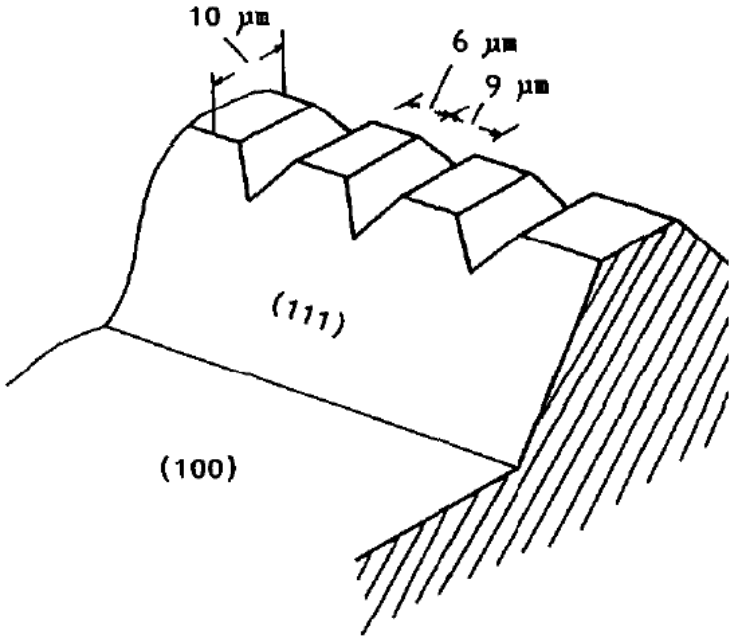

Figure 5 [14]: The V-shaped microgrooves were fabricated on silicon by wet anisotropic etching. The grooves had a length of 10 μm and an opening width of 9 μm.

Kobayashi et al. (2002) designed a droplet-based microfluidic device using silicon microfabrication methods to generate emulsion droplets. The device investigated the size of emulsion droplets created with circular and oval through-holes. Uniform through-holes were fabricated on a silicon wafer. The holes were 2 types: circular (diameter of 10 μm) and elongated (equivalent diameter of 17.3 μm). The fabrication process as shown in the figure below: a,b) A 0.2 mm aluminum layer is deposited on a bare silicon wafer. c) Photoresist is

spin coated. d) Photoresist is patterned and developed. e) Aluminum layer is etched. d) Through-holes are etched in the silicon wafer by deep reactive ion etching (DRIE) using aluminum as a protective layer. [15]

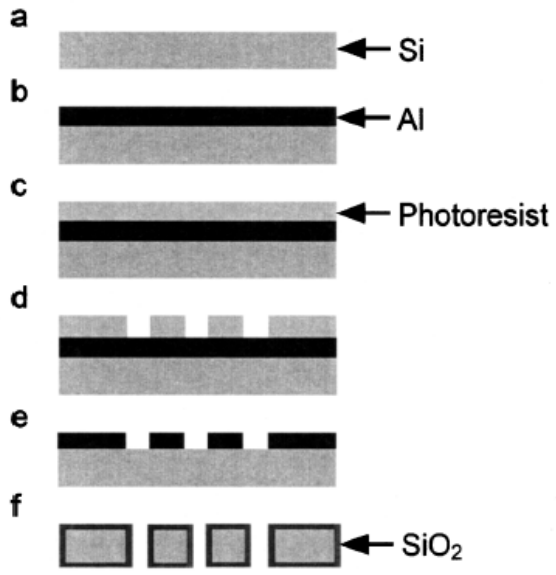

Figure 6 [15]: a,b) A 0.2 mm aluminum layer is deposited on a bare silicon wafer. c) Photoresist is spin coated. d) Photoresist is patterned and developed. e) Aluminum layer is etched. d) Through-holes are etched in the silicon wafer by deep reactive ion etching (DRIE) using aluminum as a protective layer.

The through-holes generate oil droplets, which are then dispersed and carried in a 0.3% sodium dodecyl sulfate solution that flows continuously over the chip as shown in the figure below. [15]

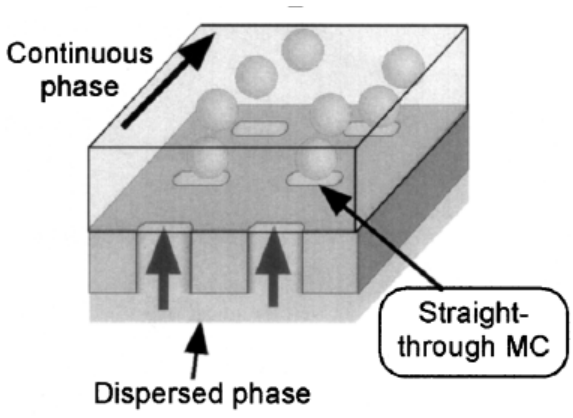

Figure 7: Generated oil droplets are carries away in a continues flow of sodium dodecyl sulfate solution. [15]

4 Microfluidic channel design with use of vacuum trenches

In Chapter 2, a general explanation was given on how microchannels are fabricated in silicon using microfabrication methods. In this chapter, two designs for a microfluidic device working with cell mechanobiology principles will be explained. Each of these designs has several versions that vary in details to find the best choice for successful microfabrication.

4-1 Pumping setup considerations

Before the start of the design, the pumping system that the microfluidic device could be connected to, had to be take into consideration. The pumping system has a plastic holder in which the microfluidic device could fit. The holder is a patch-clamp system designed by Cytocentrics B.V. The picture below shows the general design of the holder. The holder covers the top of the device and can fit in a 2.5*3 mm^2 chip. There are seven valves in the holder that can be opened by pressing a needle (circles in the figure 8). Four of these valves connect to the pumping system, acting as inlets and outlets (shown in the picture). The 3 valves in the middle are used for injecting other fluids if needed. The setup allows for observation of the chip from the back in an approximately 250*250 μm^2 area depicted in the picture.

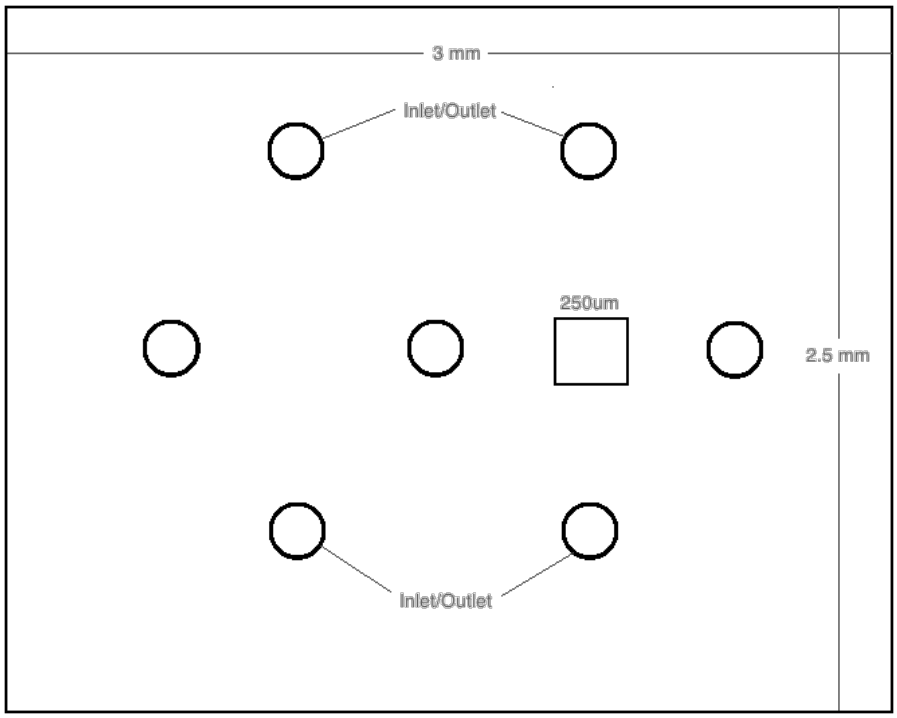

Figure 8: Holder design and dimensions

The microfluidic device should fit in the holder and the inlets, outlets and the restriction channels should be designed in the predetermined positions.

4-2 Microfluidic Device Design

There are two general designs for the microfluidic device. In type I design depicted in Figure 9, cells flow in the channels colored in black, while the medicine that must be tested flows in cyan micro-channels. Both types of channel are 50 µm wide and 40 µm deep. Cell and medicine channels run in parallel and are connected through very small pores in the silicon membrane separating them. The pores are too small for the cells to pass through, however the medicine diffuses to the cell channel due to difference in concentration. The length of the channels where they are effectively in parallel is about 28 mm.

The cells enter the device from "cell inlet" and pass through a restriction channel that has a smaller width than the cells. The time the cells take to pass through this section is measured. The cells then go through the serpentine channels that give them time to be affected by medicine that is entering the cell channel by diffusion. In the end, cells pass through a second restriction channel and the pass time is measured again and the cells exit the device through the cell outlet. Because the restriction channels have a smaller width than the cells, the cells have to deform to be able to pass through them. Diseased cells show different mechanical properties than healthy cells and the medicine can also affect these properties. The changes in pass time can indicate the effectiveness of a medicine.

The width of the restriction channel depends on the type and size of cells that are being tested. A width of 7-8 µm is suitable for monocytes (they have a diameter of 15-30 µm).

Figure 10 shows type II design. For this design we only have cell inlet, outlet and channels. In this case, the medicine flows over the device and enters the serpentine channel through the porous membrane on the top.

In both designs mentioned above, microchannels are fabricated with the method depicted in figure 6. Each channel is made of thousands of very small rectangles that are etched in the silicon wafer and then connected to each other under the surface to make one big channel. Each channel design has several versions for different rectangle sizes.

Microchannels were designed using Clewin software and transferred to a dark-field photomask with EBL[1] for lithography.

In the next section, the details of each design are given.

[1] Electron-beam Lithography

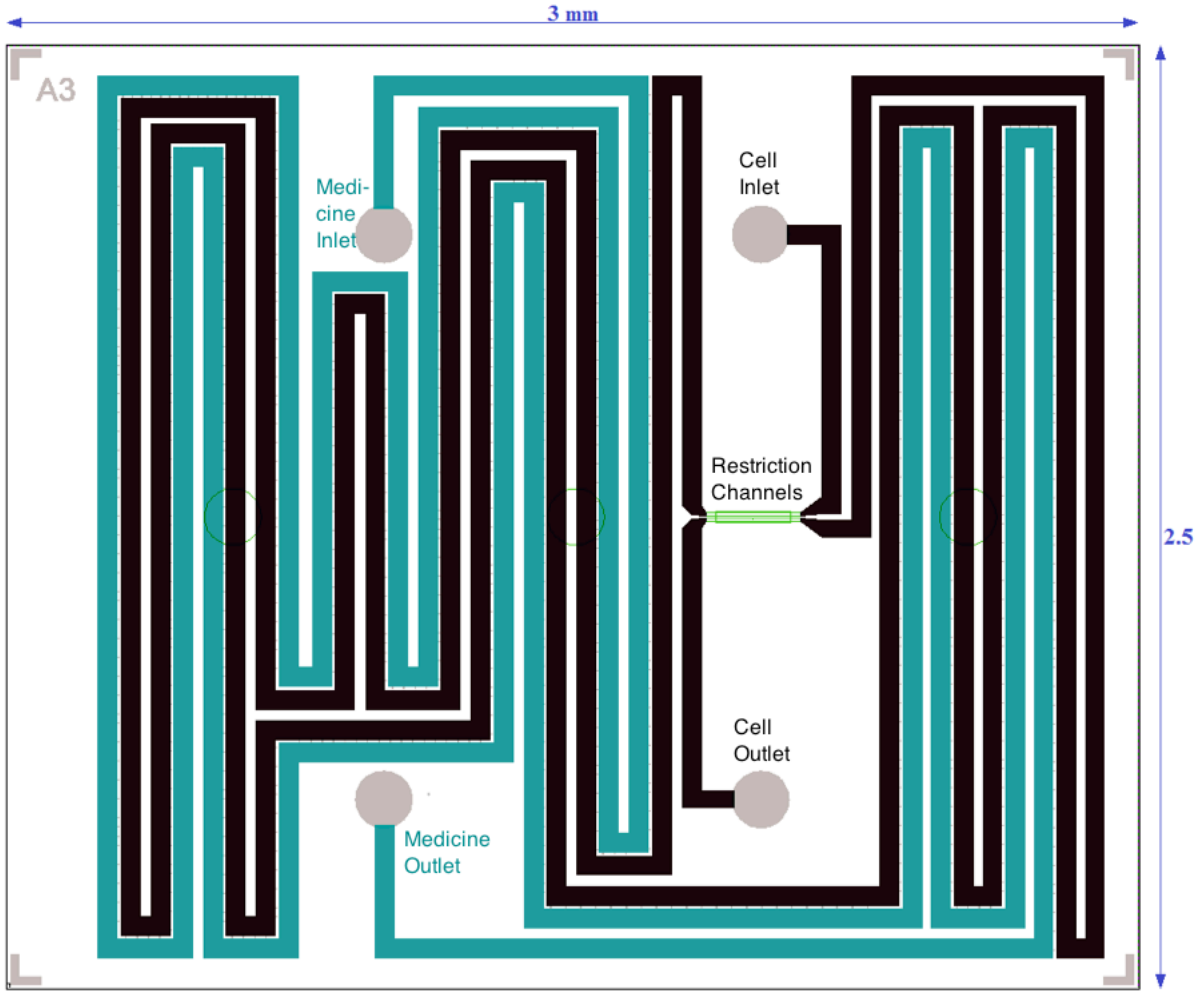

Figure 9: The cells enter the device from "cell inlet" and pass through a restriction channel that has a smaller width than the cells. The time the cells take to pass through this section is measured. The cells then go through the serpentine channels that give them time to be affected by medicine that is entering the cell channel by diffusion. In the end, cells pass through a second restriction channel and the pass time is measured again and the cells exit the device through the cell outlet.

4-3 Photo-Mask Design

The first step of silicon microfabrication process is to design and fabricate a photomask that is used in lithography to pattern the wafers. The main design is for the front of the wafer where microchannels are fabricated. However, a simple design for the back of the wafer that shows where the wafer should be etched to allow observation of restriction channels from the back, is also needed.

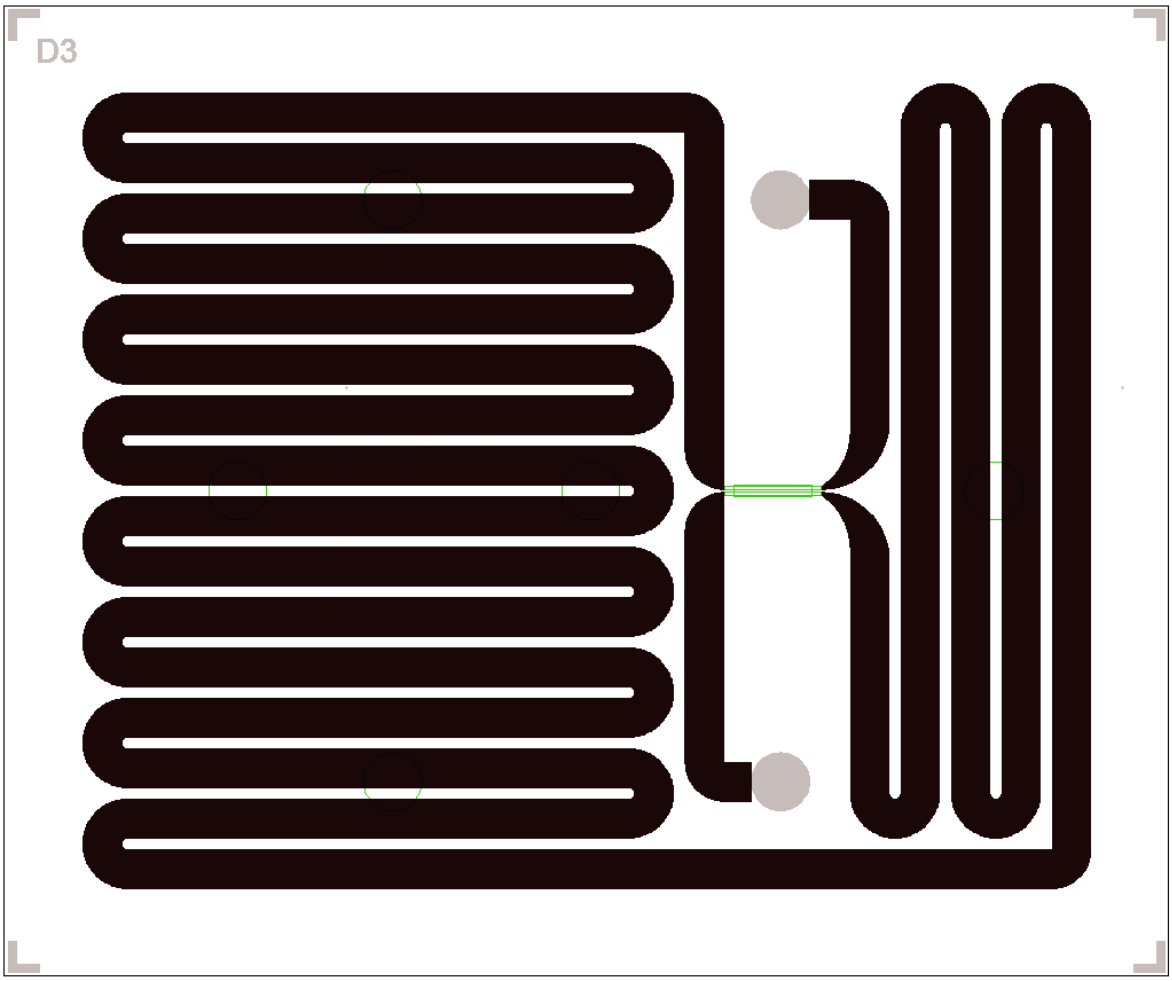

Figure 10: Type II design. Dimensions are the same as Figure 9. The features are cell inlet, outlet (gray circles) and cell channels. In this case, the medicine flows over the device and enters the serpentine channel through the porous membrane on the top.

4-3-1 Front Mask

Overall front view:

A photomask is used by a stepper machine to expose patterns on a silicon wafer. The stepper exposes a pattern on the photomask multiple times on one wafer. Each time the pattern is exposed, it is called a "die". These dies can be all exposed with the same energy and focus or have different energies and focuses. In this research, each die is made of 15 microfluidic chips with different channel designs and one section (bottom left) for testing etching times and conditions of various trench sizes and designs. The designs have been given the designations A1, A2, A3, B1, B2, B3, B4, C1, C2, C3, C4, D1, D2, D3 and D4 as depicted in figure 11. A, B and C are type I designs and Ds are type II designs. The difference between these designs is in the dimensions of the trenches. The small "L" like structures in the corners

of Figures 9 and 10 that are also visible in Figure 11 are markers used for dicing to separate the chips from each other.

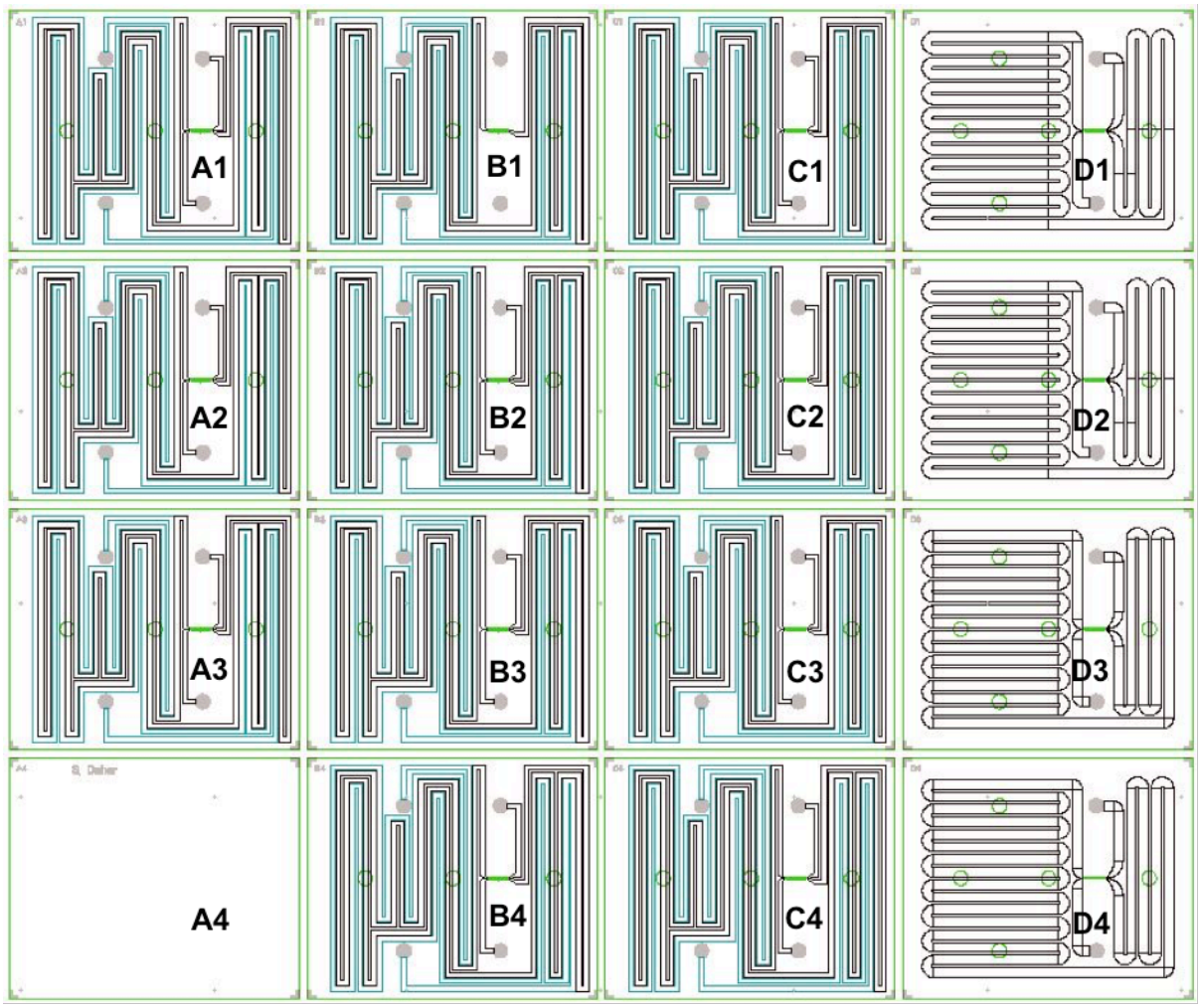

Figure 11: A, B and C are type I designs and Ds are type II designs. The whole die is 12.2*10.3 mm^2 and each chip is 3*2.5 mm^2.

Trench Variations:

Different trench sizes were designed to find out the most suitable dimensions for exposure, etching and covering. Bigger trenches are easier to expose and etch, but need a thicker layer of TEOS SiO_2 to close them. If the trenches are very close to each other (lower pitch) CF_4 etch will be shorter, but there is a possibility of two trenches connecting in the hanging SiO_2 membrane and creating a bigger trench that cannot be fully closed with TEOS. Table 1 lists the trench sizes of all designs.

Design	A	B	C1-2	C3-4	D
Trench Size	0.6 x 2.4	0.8 x 3.5	1 x 1	0.8 x 0.8	1 x 1
Pitch	1.3	1.6	1.9	1.6	1.6

Table 2: Trench and pitch sizes for various designs. All numbers are in µm.

Experiments showed that designs A and B worked best. These designs had bigger trench dimensions than C and D. The lithography was successful, the DRIE was able to reach the desired depth (40 µm) and the trenches were successfully closed with TEOS. DRIE process in designs C and D was too slow because of the small trench openings and the 0.5 µm thick SiO_2 membrane was all lost during 40 µm silicon DRIE. Increasing the thickness of photoresist to protect SiO_2 better was also not possible because of exposure difficulties. Designs C and D however would work for a BOX layer that is buries 20µm deep instead of 40 µm.

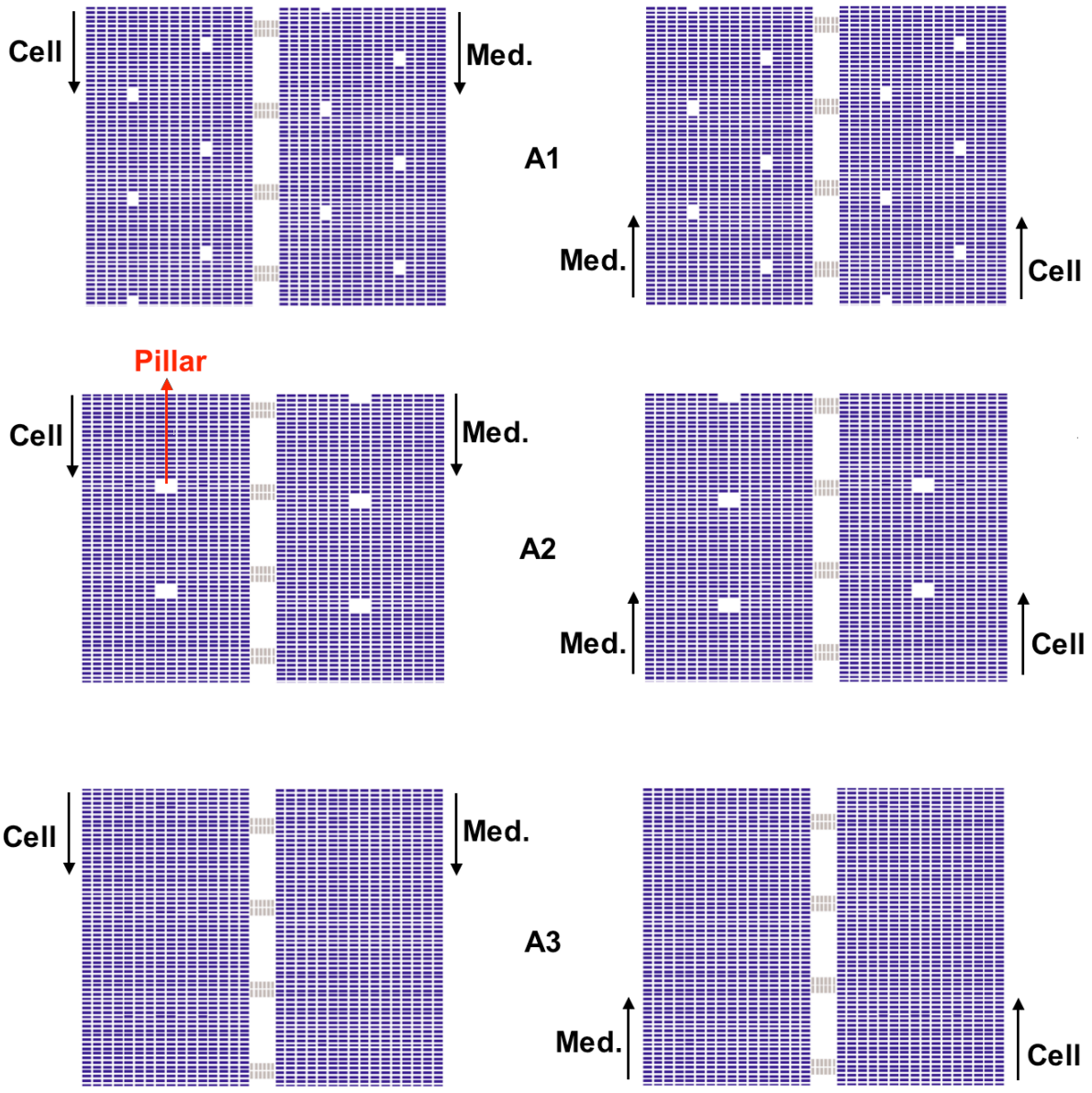

Figure 12: Designs A1, 2 and 3. Each row shows two pairs of microchannels. Blue rectangles are the trenches making up the microchannels and gray rectangles are the trenches creating the pores. Flow directions and pillars/mixing structures are also indicated. Trench size: 0.6*2.4µm.

Figures 12 to 15 show designs A to D. In Figures 12 and 13, each row shows two pairs of microchannels (4 microchannels). Each pair of microchannels has one channel for cells, and one for medicine and these channels are connected with pores (gray in the pictures). Directions of the flows are depicted with arrows. In figures 12 to 15, the small blue and gray rectangles are the trenches that are exposed during lithography (look at Figure 3-e). The white areas in the middle of the channels, show an absence of trenches. The wafers are not exposed or etched in these areas, resulting in creation of pillars inside the channels. These pillars hold up the SiO_2 membrane and they can also create turbulences and function as passive mixing structures.

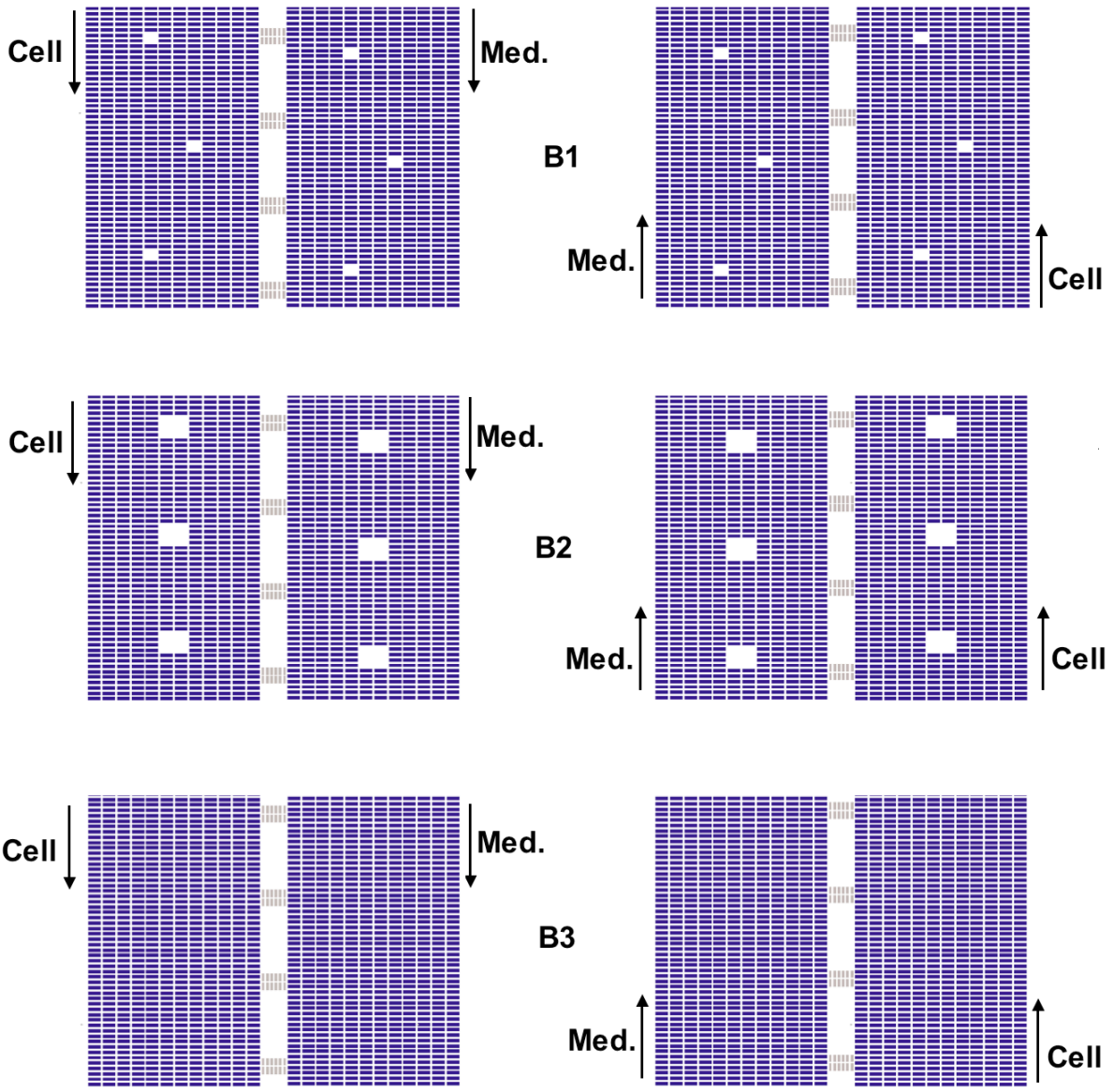

Figure 13: Designs B1, 2 and 3. Each row shows two pairs of microchannels. Blue rectangles are the trenches making up the microchannels and gray rectangles are the trenches creating the pores. Flow directions are also indicated. Trench size: 0.8*3.5 μm^2.

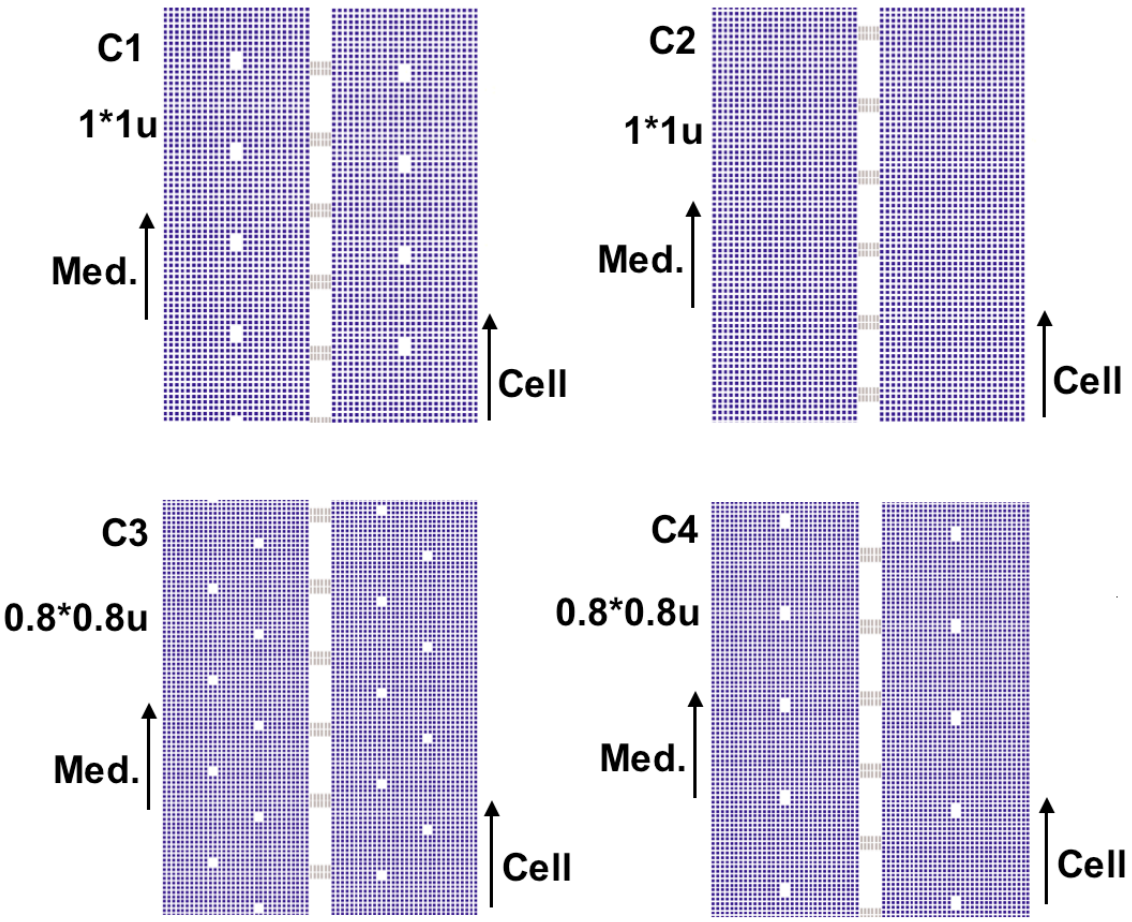

Figure 14: Designs C1, 2, 3 and 4. Blue squares are the trenches making up the microchannels and gray rectangles are the trenches creating the pores. Flow directions and pillars are visible. Trench size: 1*1 μm^2 for C1&2 and 0.8*0.8 μm^2 for C3&4.

In designs A, B and C, each channel is 50 μm wide and there is a 10 μm distance between connected cell-medicine channel pairs. Each pore is about 4.5 μm wide.

Figure 15 shows D designs. These designs only have cell channels (Figure 10). White areas in the middle of the channels are pillars, while the bigger blue squares are large trenches that are not closed with TEOS. They create pores on the top membrane that allow for medicine flowing over the microchannels to enter them. (Also look at Figure 33.)

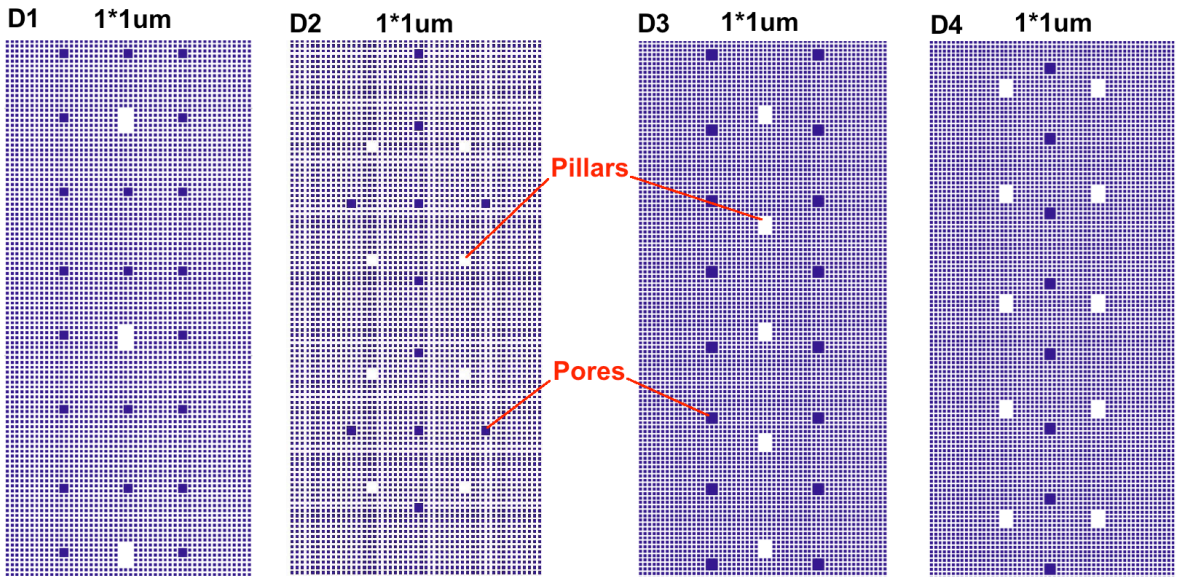

Figure 15: Designs D1, 2, 3 and 4. Blue squares are the trenches making up the microchannels. Pillars and pores are indicated in the picture. Trench size: 1*1 μm^2.

Restriction channels:

All designs have 2 restriction channels in a specific place (pre-determined by holder design). Figure 16 depicts the restriction areas in design A. The green lines are guidelines that are not printed on the photomask. In the figure, each restriction channel has dimensions of 7.5*250 μm^2 and there is an 8 µm distance between the input and output channels.

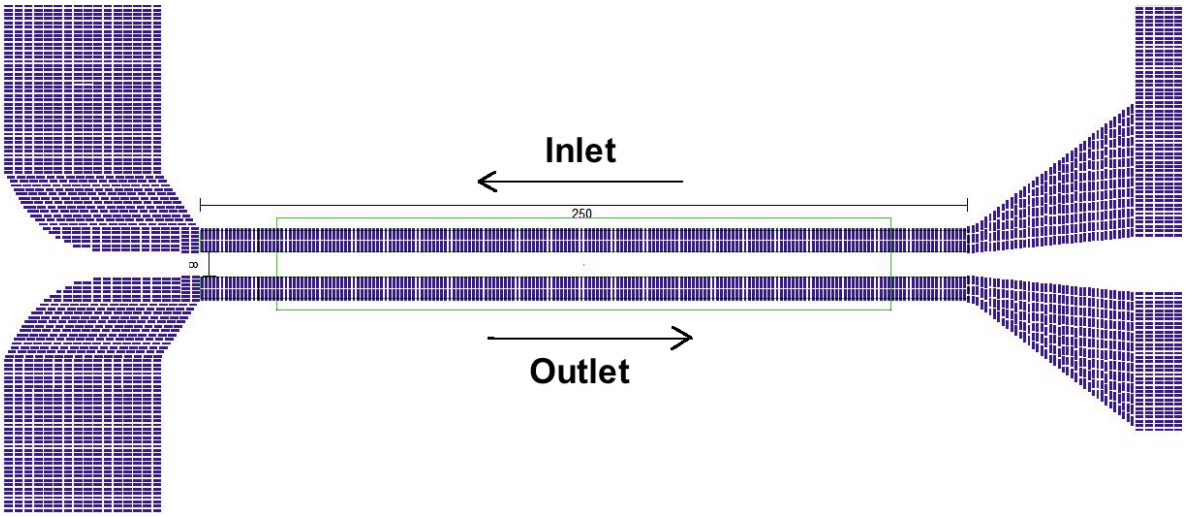

Figure 16: 7.5*250 μm^2 restriction channels.

4-3-2 Backside

The mask designed for the back of the wafer is simple with one single feature: A 250*250 μm^2 square that is placed right behind the restriction areas.

In the picture below, the green lines show the borders of the chip and the borders of each design (A1, 2, 3, etc.). They are not transferred to the photomask. Gray squares indicate observation areas.

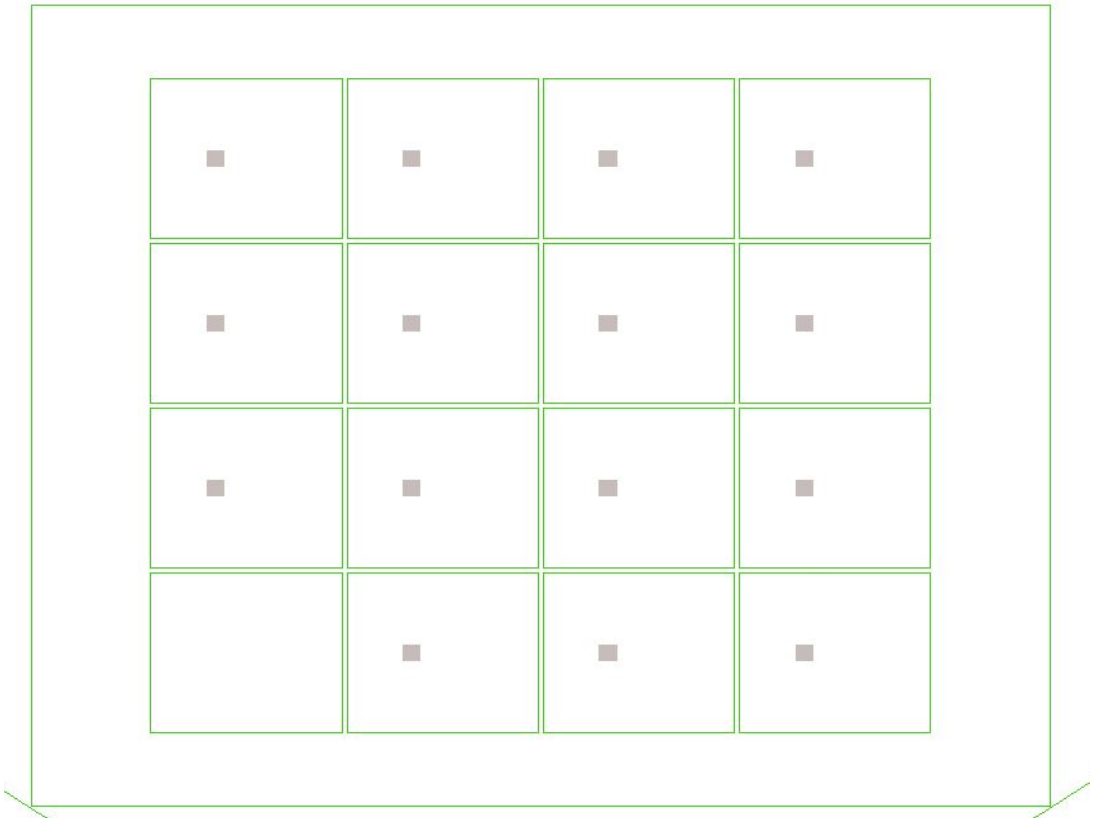

Figure 17: Backside mask. The gray square indicates the observation area.

After the mask has been fully designed (using CleWIN mask design software), the patterns are transferred to a dark-field photomask with Electron-Beam Lithography (EBL).

5 Microfluidic channel fabrication

A list of tools and processes of microfabrication of front side of the wafer has been included in the Appendix at the end of this document.

5-1 Cleaning Wafers

The very first step after opening a box carrier containing a new batch of silicon wafers, is cleaning the wafers before the start of the process. The surface of the wafer is contaminated after being kept in a plastic box carrier for a long time. A cintillio cleaning tool was used for this purpose.

Cleaning process: HydrOzone (O_3:H_2O) combined with FluorOzone (HF) is used for cleaning particle contaminations and passivating oxide films. HydroOzone oxidizes a very thin layer on the surface of the wafer and at the same time HF removes the oxide, then the wafer is rinsed. The cycle of etching and rinsing continues for about 25 minutes. [18] Figure 18 depicts an overview of the cleaning mechanism of Cintillio.

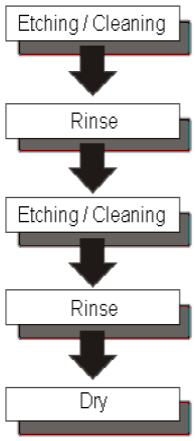

Figure 18 [18]

5-2 Silicon Dioxide Deposition

After cleaning the wafers, a layer of silicon dioxide with thickness of 0.5 µm is deposited on the wafer. Layer deposition induces stress on the wafer. Too much stress will result in a big curvature in the wafer and prevent further processing, so the wafer should be put under as little stress as possible. The method chosen for SiO_2 deposition was Plasma Enhanced Chemical Vapor Deposition (PECVD). At 400°C the deposition parameters have been optimized to deposit a dioxide layer with the minimum possible stress (almost zero). [7]

Choosing SiO_2 layer thickness:

In previous experiments with vacuum trench fabrication, a photomask with bigger features than the mask designed for microfluidic channels was used. Smaller features require a thinner layer of photoresist for exposure. Considering the pattern sizes, the photoresist layer that was used could not be thicker than 1 µm. On the other hand, photoresist acts as a masking layer

for dry etch of SiO_2. Some photoresist is lost during SiO_2 etch, so if the dioxide layer is too thick, then all photoresist will be lost before the etching of SiO_2 is complete. Two dioxide layer thicknesses (0.5 μm and 0.7 μm) were tested. 0.5 μm of SiO_2 gave better results: About 0.8 μm of SPR photoresist was lost during dry etch of 0.5 μm of SiO_2.

Induced Stress:

Figure 19 shows how the stress of a substrate induced by a deposited film is calculated from the curvature of the substrate and the film thickness. [8]

In Figure 19: Stress $\sigma = \frac{Eh^2}{(1-\nu)6Rt}$, where [19]:

- "$\frac{E}{(1-\nu)}$" is the biaxial elastic modulus of the substrate (1.805×10^{11} Pa for <100> silicon wafers).

- "h" is the substrate thickness (m);

- "t" is the film thickness (m);

- "R" is the substrate radius of curvature (m): $R = \frac{R_1 R_2}{R_1 - R_2}$ (R_1: Radius before thin film deposition and R_2: Radius after thin film deposition).

Now stress σ is calculated. A negative sign indicates compressive stress and positive sign tensile stress.

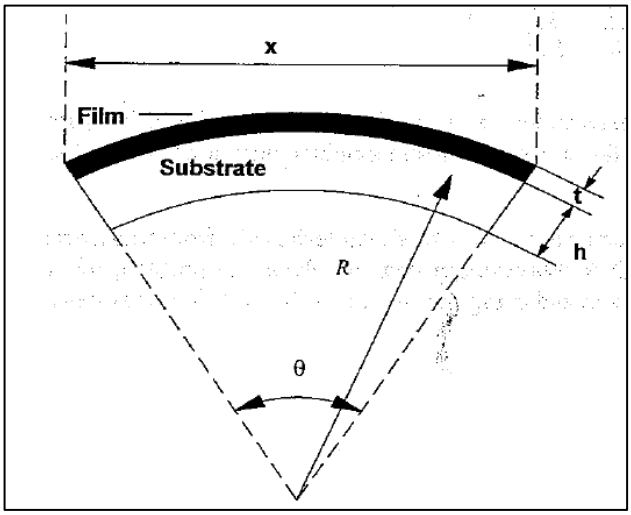

Figure 19 [19]

Figure 20 shows a wafer's curvature and stress as after 0.5 µm PEVCD dioxide and 1.5 µm TEOS deposition as measured by Flexus [8]. The measured stress is -58 MPa, which is a low stress as was desired. The mentioned "bow" of the wafer is the difference between the lowest and the highest point on the wafer surface. Bare wafers typically have a horizontal s-shaped curvature that indicates a small bow.

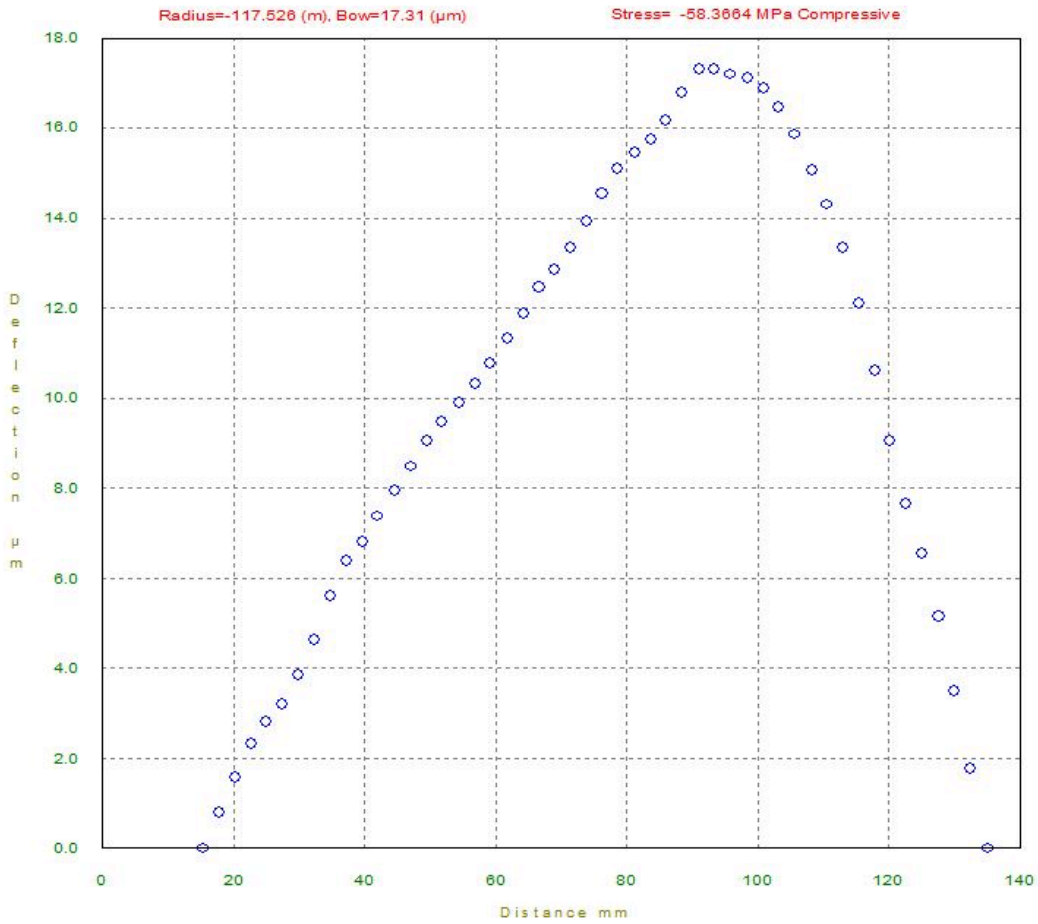

Figure 20: The figure shows the curvature of an SOI wafer with both PECVD and TEOS SiO_2 layers. Stress and bow are both indicated. The stress is low as was desired. Stress = -58 MPa. [8]

5-3 Lithography

A layer of positive photoresist is deposited on the wafer. The patterns making the microchannels are transferred from the photomask to the silicon wafer with lithography.

Lithography: Photoresist is exposed to the patterns using a stepper. The photoresist is then developed and the areas that were exposed are dissolved in the developer and removed while non-exposed areas remain and the pattern is transferred (Figure 21).

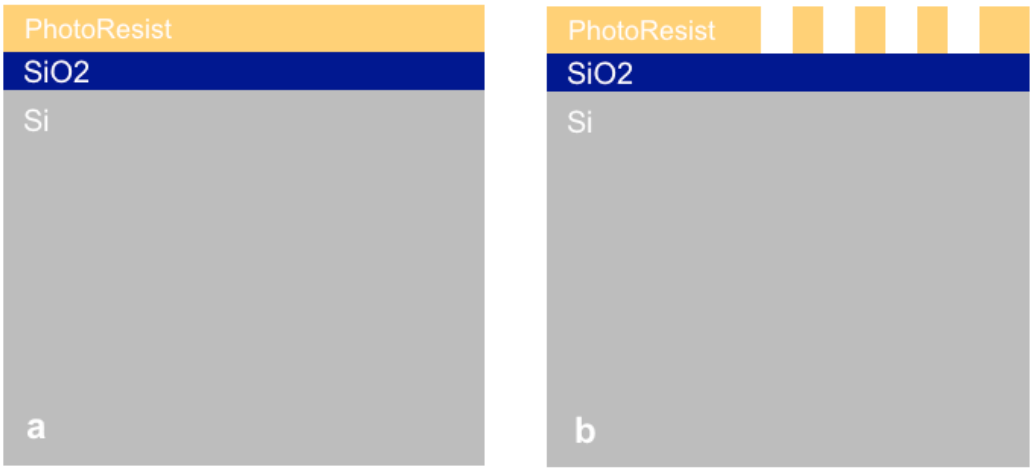

Figure 21: a) Layer deposition: SiO_2 PECVD and photoresist coating. b) Lithography.

5-3-1 Photoresist thickness

Photoresist thickness is a compromise between masking capability during etching and exposure resolution.

- The photoresist cannot be too thick. The biggest patterns in the photomask were 0.8*3.5 μm^2 rectangles, while the smallest patterns were 0.8*0.8 μm^2 squares. The photoresist used could not be too thick as exposing such small features would be impossible.

- The photoresist cannot be too thin. The photoresist must be thick enough to survive at least the dry etching of the SiO_2.

A 0.8 µm thick layer of SPR660, a positive photoresist, was used for lithography in these experiments. The layer was completely lost during the SiO_2 dry etch. In the last experiments, a slightly thicker layer of resist was used (1 µm) which resulted in a few nanometers of resist remaining after SiO_2 dry etch. The remaining resist was lost during silicon DRIE.

5-3-2 Exposure and Development of Photoresist

Several energy/focus matrixes were tried to determine the best energy and focus for exposure. Energy/focus matrix is a change of exposure energies/focus heights over different dies in one

wafer. Different pattern sizes showed compatibility with different exposure parameters. I decided to focus on the bigger pattern in designs A and B. The best results were achieved for:

Designs A1, 2 and 3: 240 mj/cm^2 energy and -0.4 µm focus.

Designs B1, 2, 3 and 4: 220 mj/cm^2 energy and -0.4 µm focus.

After exposure, the wafer is developed in SPR developer. Developer is a solvent that dissolves and removes parts of the resist that have been exposed while the unexposed parts remain untouched.

SPR660 needs a DESCUM step after development to remove possible remaining photoresist residues from the bottom of exposed areas. The DESCUM performed was a 2 minutes O_2 plasma etch at 90°C in a barrel.

5-4 Deep Reactive Ion Etching (DRIE)

After the patterns are exposed and developed in photoresist, the exposed areas are plasma-etched. First the dioxide layer is etched using He, CF_4 and H_2 (end point detection on silicon). Then trenches are etched inside silicon with Deep Reactive Ion Etching (using the Bosch process). All the photoresist is lost during etching processes. The SiO_2 layer acts as masking layer for most of silicon DRIE, resulting in loss of some of the layer.

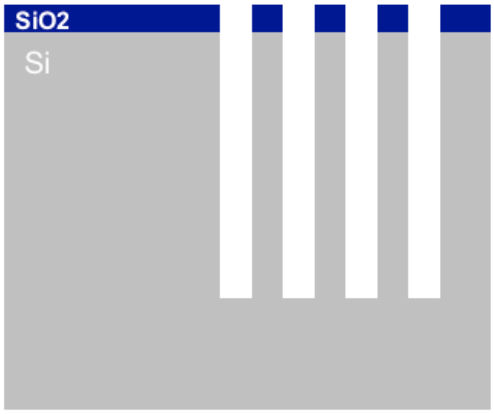

Figure 22: Schematic of DRIE

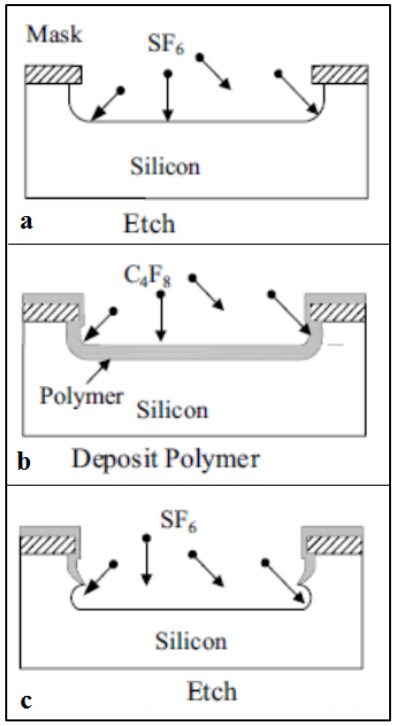

Figure 23: Bosch Process

Bosch Process: Deep etching with repeated cycles of etching and passivation. First the silicon is etched with a mix of SF_6 and 10% O_2, and then the sidewalls are passivated with C_4F_6. The cycle is then repeated (Figure 23). Longer cycles mean faster etch rate but bigger scallops on the sidewalls. The size of the opening in the mask directly influences the speed of DRIE. Very small opening in the mask results in the etch rate decreasing rapidly as we go deeper in the wafer. This is the reason designs C and D failed to reach the BOX layer during DRIE. Figure 34 shows the difference in DRIE speed in an inlet and microchannels.

5-4-1 Notching effect on SOI wafers

Figure 35 shows a microfluidic device with design B3 fabricated on SOI wafer and covered with TEOS SiO_2. DRIE on a SOI wafer results in a notching effect in inlet and outlets. The notching effect is the opening of a narrow horizontal groove (the "notch") in the silicon at the interface with an underlying insulator (The buried dioxide layer in an SOI wafer) due to local charging of the insulator that guides the bombarded ions towards the conductive sidewalls [21]. The notching effect happens due to over-etch during DRIE. If all the patterns to be etched do not have the exact same dimensions, they will not be etched at the same rate. Inlets and outlets are etched faster than the channels and notching occurs. However the notching effect in this case is not sever enough to hinder the work of the microfluidic device.

5-5 Isotropic Etch of Silicon

Now that the trenches have been etched into silicon, the thin sidewalls between trenches must be removed to form the microchannels as shown in Figure 24.

Silicon sidewalls can be removed with isotropic CF_4 plasma etch, but before that, the passivation layer on the sidewalls that is remaining from Bosch process must be removed. O_2 plasma etching for 10 minutes with RF power of 350 W and the initial temperature of 100°C in a barrel can remove the passivation layer. Then CF_4 etch is performed. CF_4 plasma etch in a barrel is a process that is very difficult to control due to temperature increase during the process and loading effect. Under-etching with CF_4 results in failed removal of sidewalls, and over-etching results in loss of SiO_2 net hanging over the microchannels. Figure 25 shows the results of over or under-etching.

Figure 24: Schematic of Silicon isotropic etch

Temperature in CF_4 plasma etch: Increase in temperature results in increase in etch rate. In the first experiments, CF_4 etch was initiated at room temperature. It was noted that with a RF power of 450 W, the temperature would rise with time and level off at about 130-135°C. Heating the wafer with N_2 plasma (N_2 does not etch either Si or SiO_2) and starting the CF_4 etch with an initial temperature of 130°C results in a relatively stable temperature and thus etch rate.

Loading effect: To observe the results of either DRIE or CF_4 plasma, SEM[1] pictures of cross section of microchannels had to be taken. Hence, wafers had to be broken. During experiments, several times instead of a full silicon wafer, pieces of wafer were put in the barrel for CF_4, resulting in different timings for isotropic silicon etch. In the end, the suitable timing and power for removing sidewalls in designs A and B in 1 silicon wafer exposed with exposure energy of 220 mj/cm^2 was found out to be:

10 minutes in barrel with 50 mTor pressure and 450 W RF power and 130°C initial temperature.

Figure 26 shows a SEM photo of a wafer that was broken after CF_4 etch to make the trenches visible. The picture shows a cross-section of connected microchannels of design A3. The wafer in the picture is a test wafer and does not have a BOX layer. Scalps of Bosch process are visible in the bottom of the microchannels. The pores connecting the cell and medicine channels are also visible.

[1] Scanning Electron Microscopy

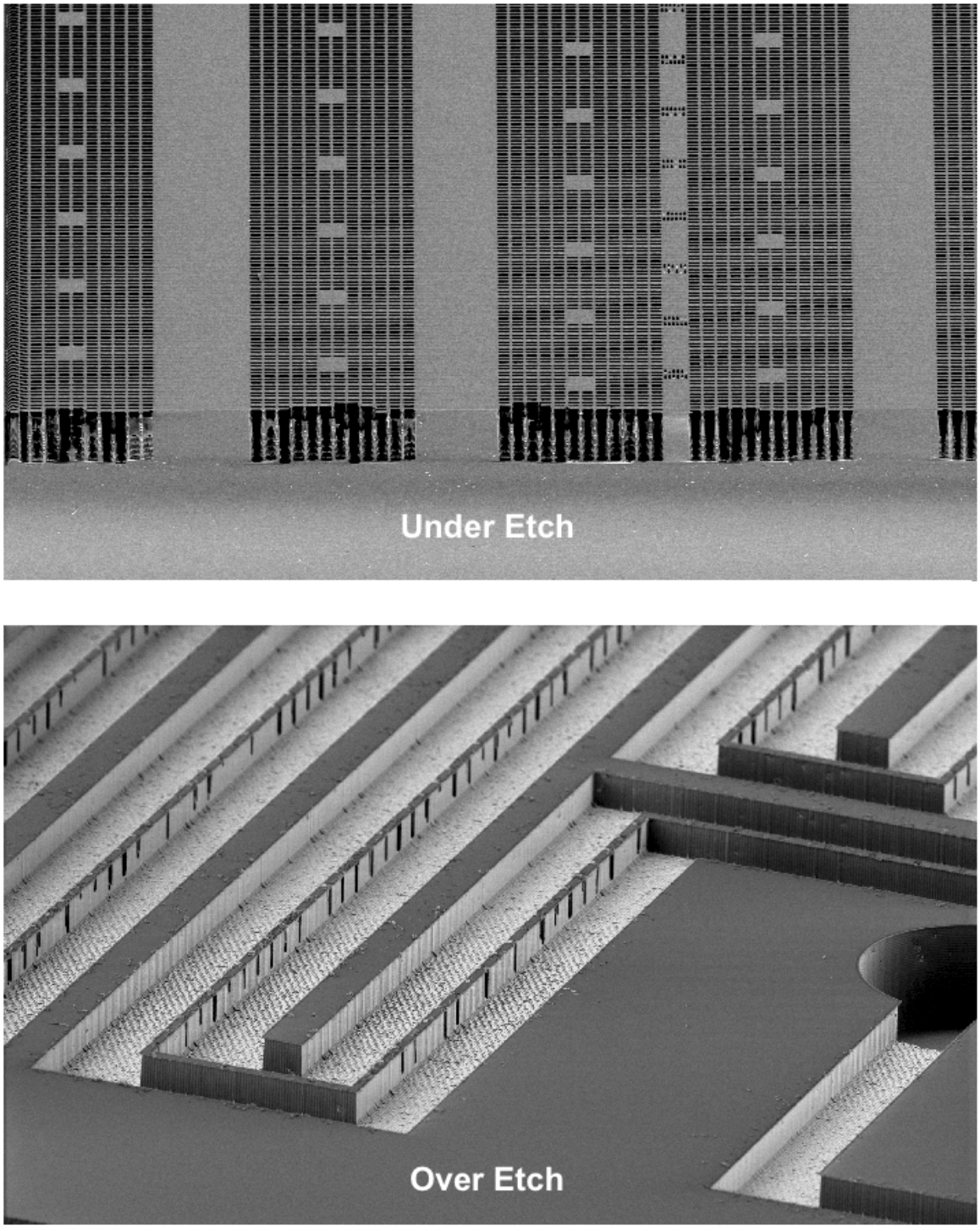

Figure 25: Under-etching with CF_4 results in failed removal of sidewalls (top picture, B2 design) and over-etching results in loss of SiO_2 net hanging over the microchannels (bottom picture, B3 design).

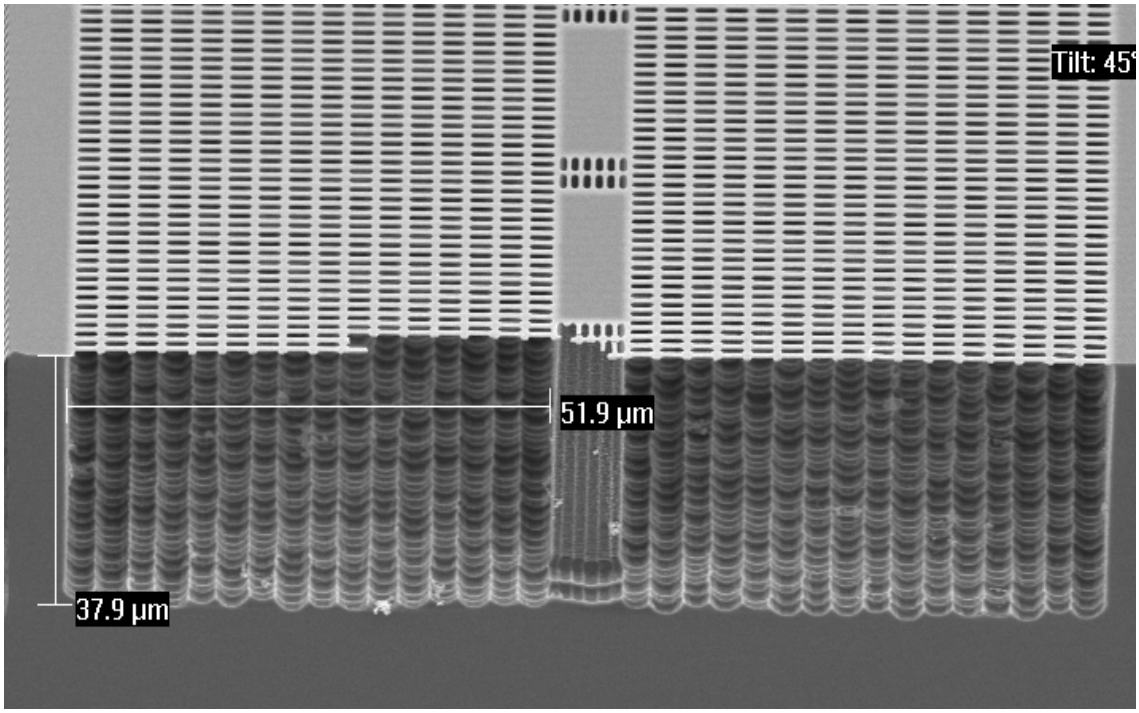

Figure 26: A cross-section of microchannels of design A3 (no pillars) that are connected by small opening in the silicon wall separating them to allow diffusion of medicine. The width and depth of each channel are indicated on the figure.

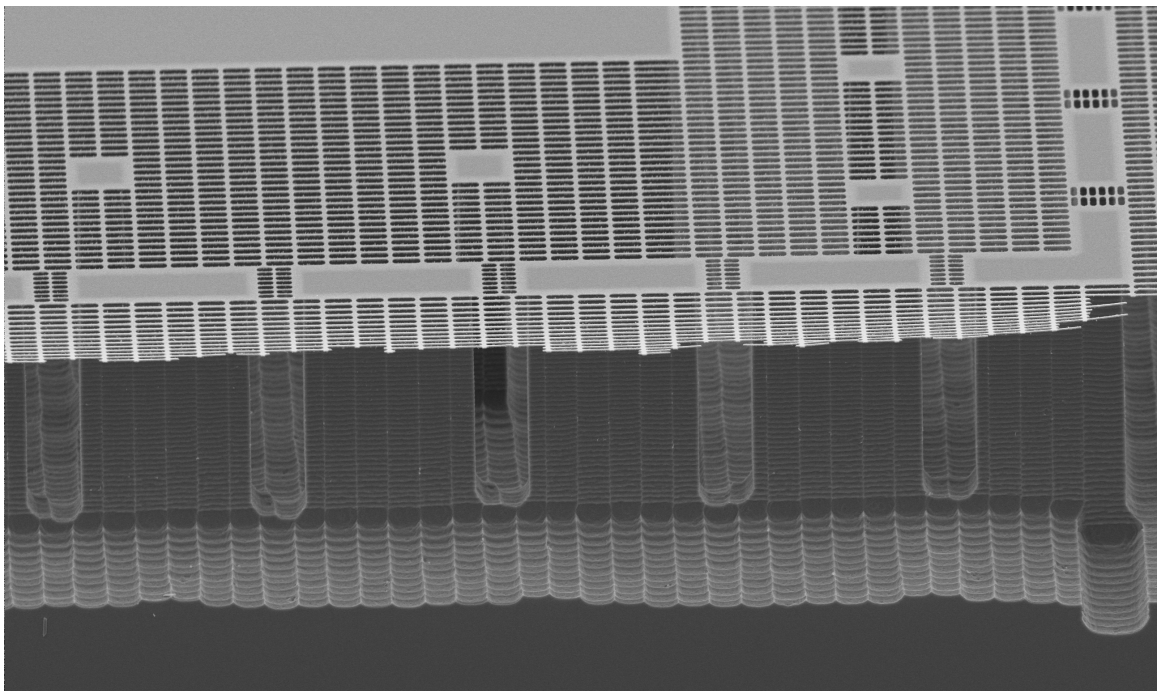

Figure 27: A cross-section of design B2. Microchannels and the pores connecting them are visible. No BOX layer.

5-6 Covering The Trenches

After the silicon sidewalls have been removed, the openings in the dioxide membrane must be covered as shown in Figure 28.

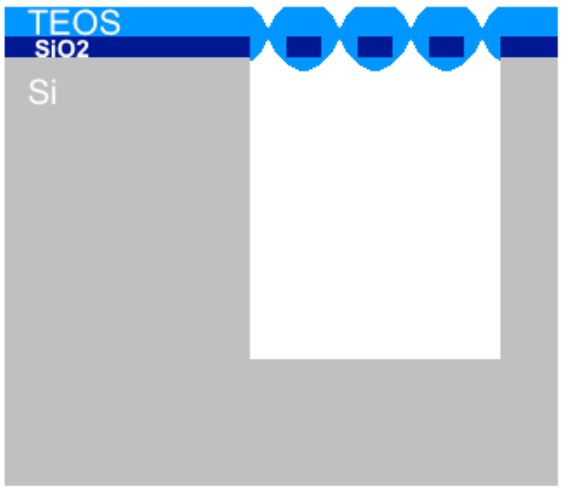

Figure 28: Schematic of covering the microchannels using TEOS SiO_2. In the figure, the dark blue layer is the original PECVD SiO_2 layer and the light blue layer is TEOS.

Covering the trenches was attempted using both PECVD SiO_2 and LPCVD TEOS SiO_2. TEOS SiO_2 is deposition of LPCVD SiO_2 by using tetraethylorthosilicate as silicon source [20]. TEOS dioxide showed better coverage (trenches that are coverable with 1.5 µm TEOS need about 2.5 µm PECVD to be closed). The disadvantage of TEOS however, is that it is a very slow method in comparison to PECVD and introduces more stress.

The figure below shows a close-up cross-section of TEOS covering the hanging SiO_2 membrane.

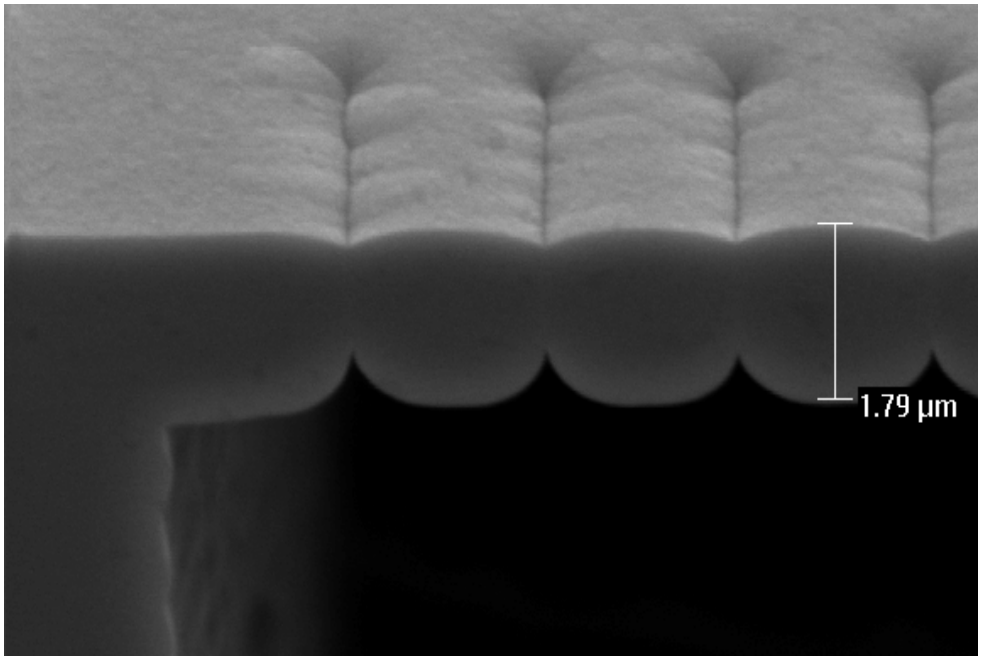

Figure 29: Cross-section picture of 1.5 µm TEOS SiO_2 closing a microchannel (design A3).

5-7 Backside Process

After microchannels have been covered on top of the wafer, the backside of the wafer is processed to open the observation area under restriction sections. First, lithography is performed with 2 µm HPR504 as photoresist. Then using the resist as a masking layer, 1.5 µm of TEOS SiO_2 and 1 µm of thermal SiO_2 are etched. TEOS is a deposition process that covers both sides of the wafer and the thermal dioxide is already present on the back of all SOI wafers. After dioxide etch, silicon DRIE is performed until it stops on BOX layer. Now the BOX layer (1 µm of transparent SiO_2) separates the restriction areas from observation hole. Cells crossing the restriction sections can be easily observed with a microscope.

Figures 30 shows the cross section of a B1 design where microchannels have been covered by 1.5 µm TEOS.

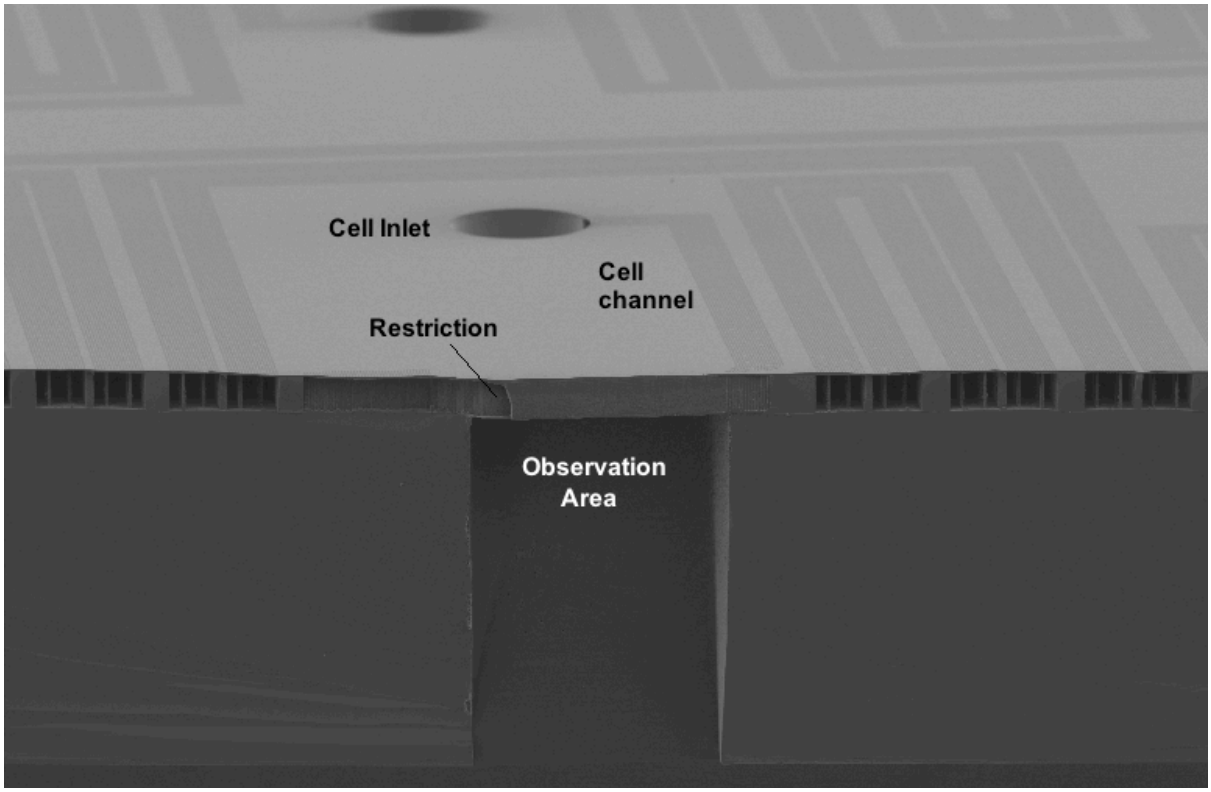

Figure 30: Cross section of a B1 design where microchannels have been covered by 1.5 µm TEOS. Inlet, microchannels, restriction section and observation areas have been indicated in the picture.

Figure 31 shows the observation area from the back of the wafer. The restriction channels are visible. The opening of the observation area is a 250*250 μm^2 square. Figure 32 is another cross-section (on a test wafer without BOX layer) and Figure 33 is a top view of design D1

covered with TEOS. Figure 34 is a SEM photo before TEOS deposition and we can see how DRIE rate changes depending on the mask opening.

Dicing:

When the fabrication is complete, the wafer is diced and each microfluidic device is separated and can now be fit into the holder of the pumping system. Figure 36 shows several microfluidic devices that have been diced from the same wafer.

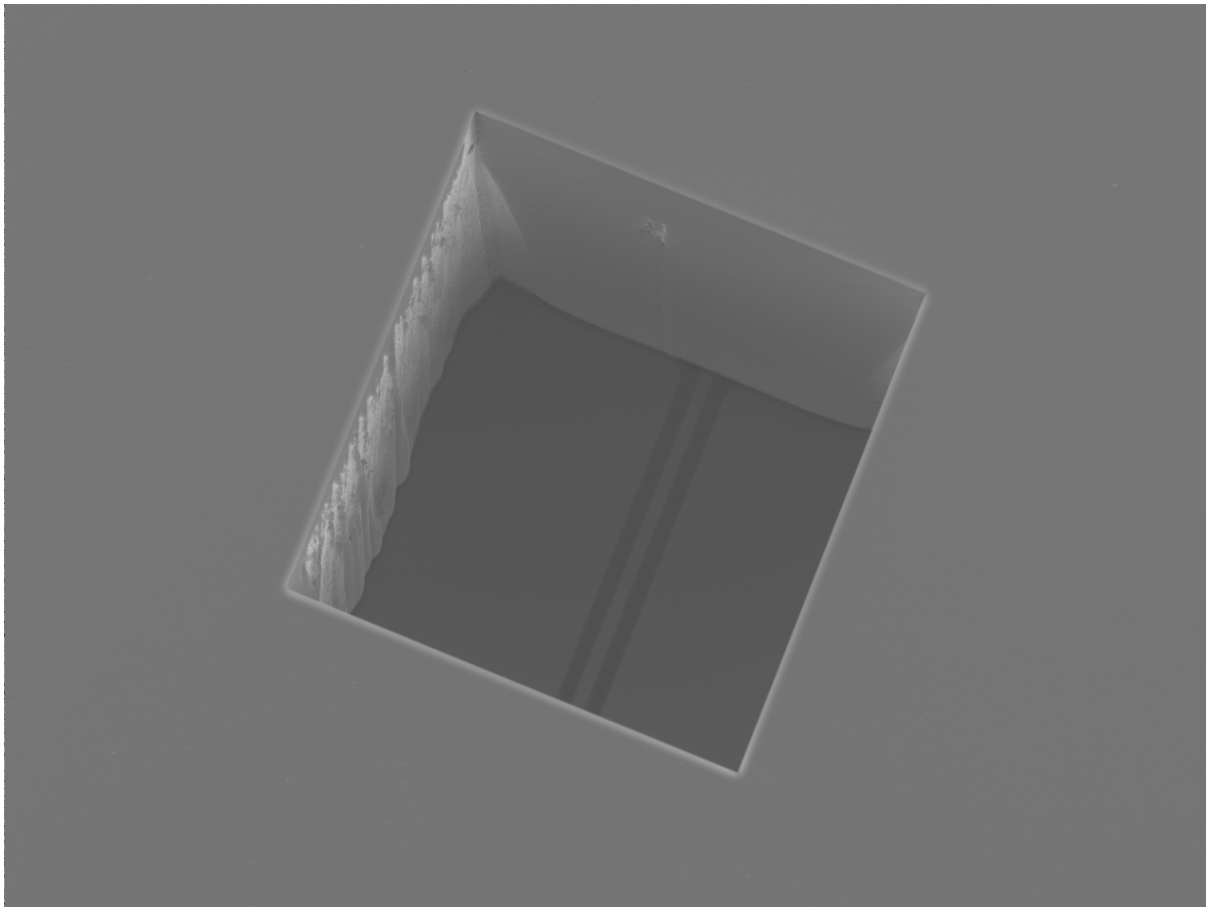

Figure 31: Observation area on the back of the wafer. Restriction channels are visible.

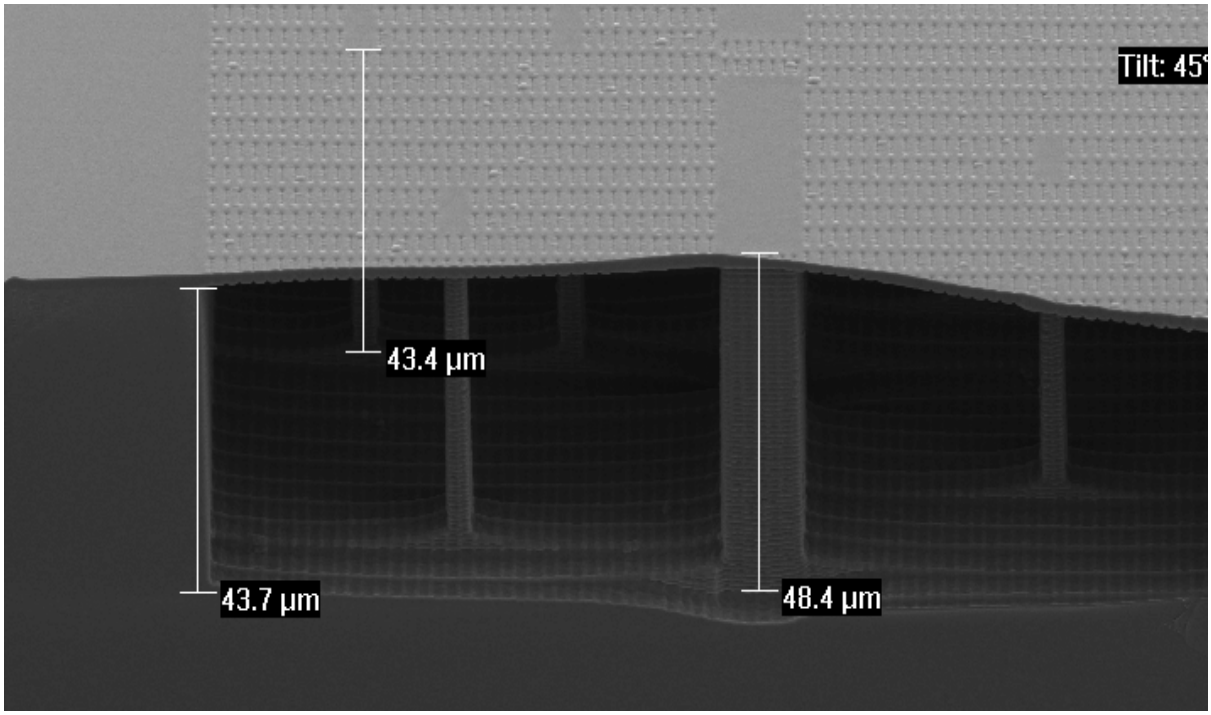

Figure 32: The picture shows microchannels of A1 design closed with 1.5 µm TEOS. The wafer does not have a BOX layer. DRIE was performed as timed etch. The channel depth is about 43 µm and the pillars in A1 design are also visible.

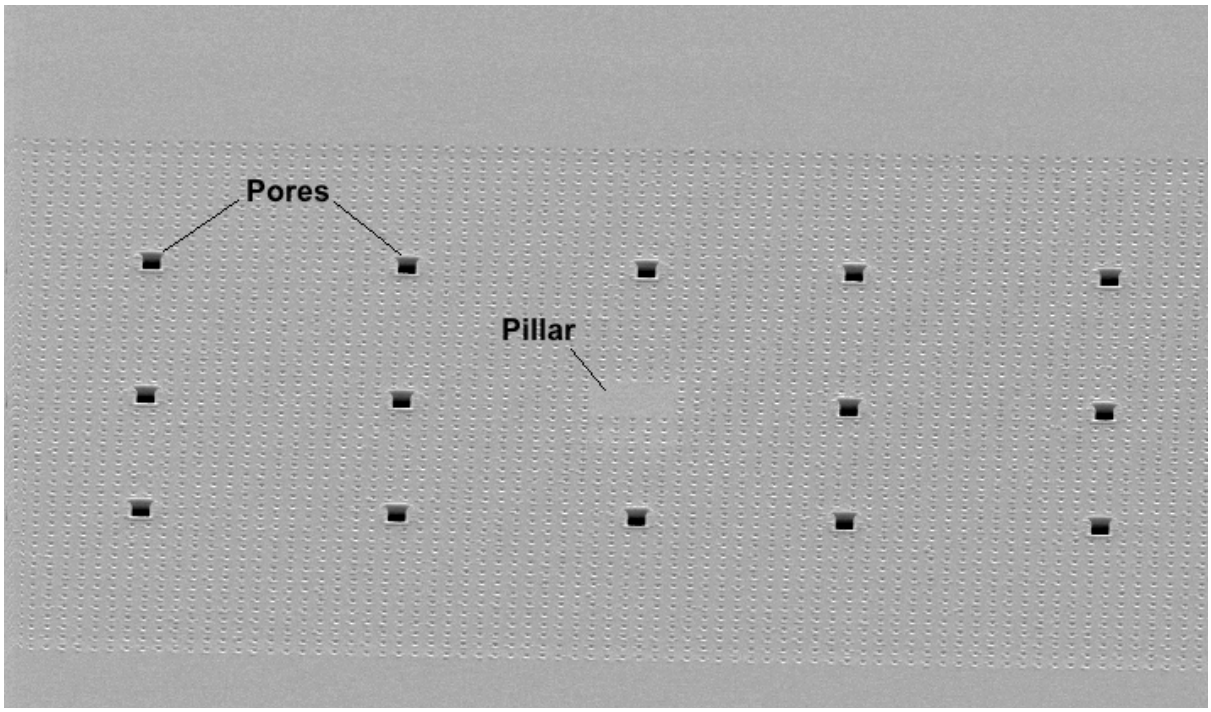

Figure 33: Top view of design D1 covered with TEOS. The pores opening above the channels allow for medicine to enter the microchannels.

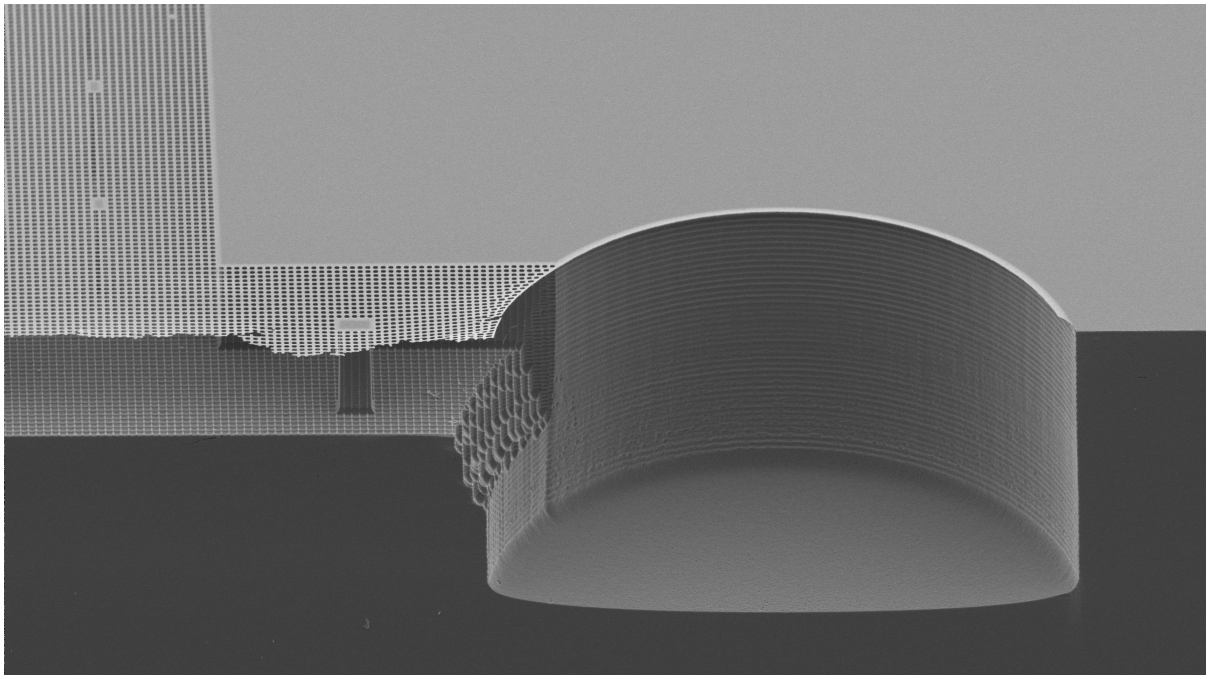

Figure 34: Size of the opening in the mask directly influences the speed of DRIE. Here we can see DRIE works faster and goes deeper in inlet and outlets.

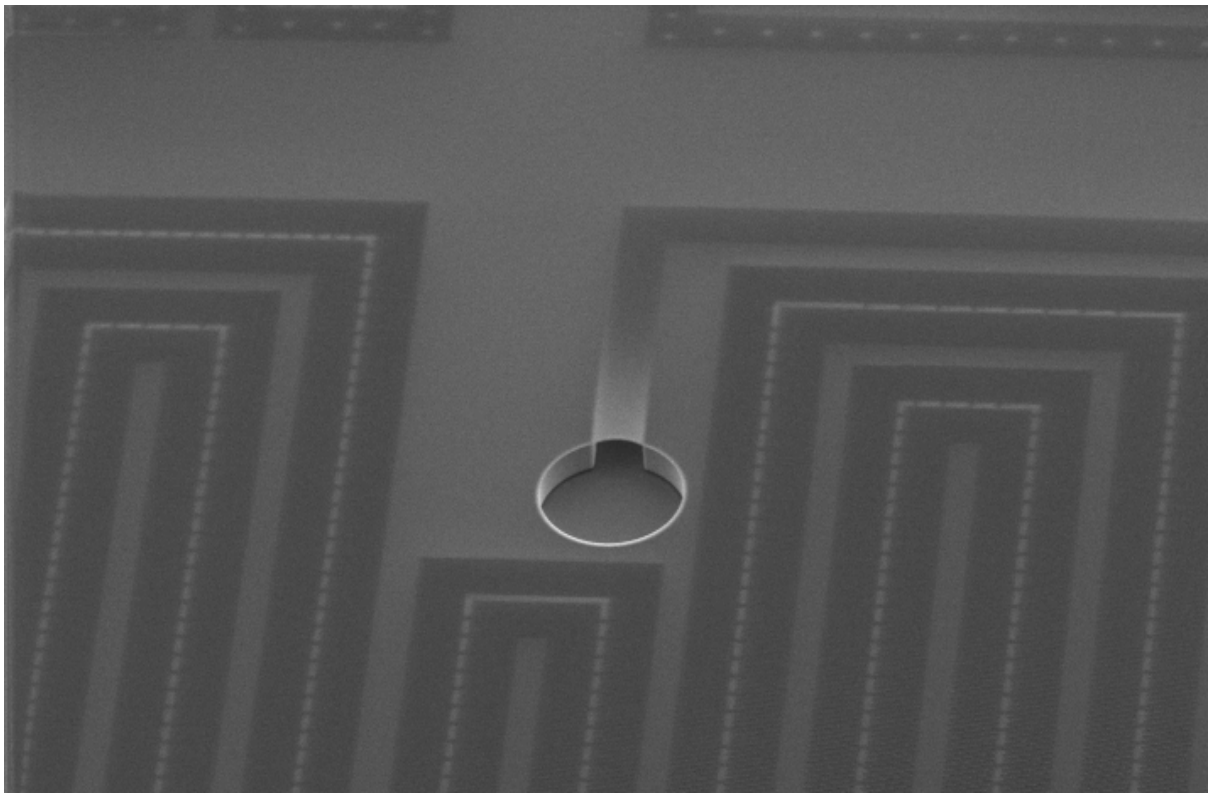

Figure 35: MF device with design B3 fabricated on SOI wafer and covered with TEOS SiO_2.

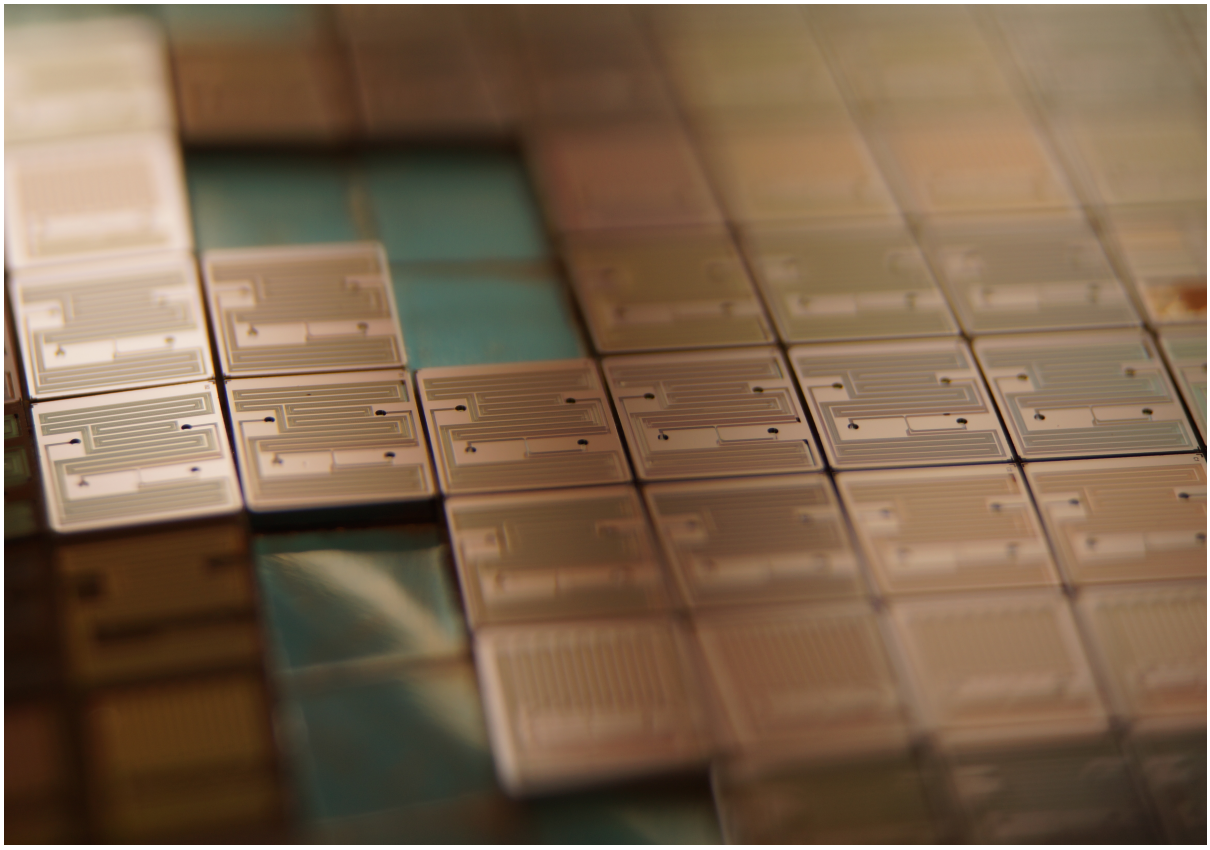

Figure 36: Microfluidic devices fabricated on the same wafer

5-8 Redesign by R.J.M. Henderikx

At the time of this research, the fabricated microfluidic devices could not be tested as a pumping setup was being built. But later tests performed by R.J.M. Henderikx indicated some design problems. Henderikx used the fabrication method developed in this research to redesign a new version of the microfluidic device of Figure 9. Henderikx's device (Figure 37) has a few changes in design. The main change is that Hendrikx's device has restriction sections in both cell and medicine microchannels to prevent a net flow that was observed from cell channel to medicine channel due to higher flow resistance in cell channel. [23]

Hendrerikx investigated the effects of Cytochalasin-D (an actin disrupting agent that weakens the cell cytoskeleton) on diseased monocytes (human promyelocytic leukemia HL60 cells). Henderikx measured the transit velocity of treated and non-treated cells. The results showed a clear distinction in velocity between non-treated cells and cells treated by Cyto-D (higher velocity). [23]

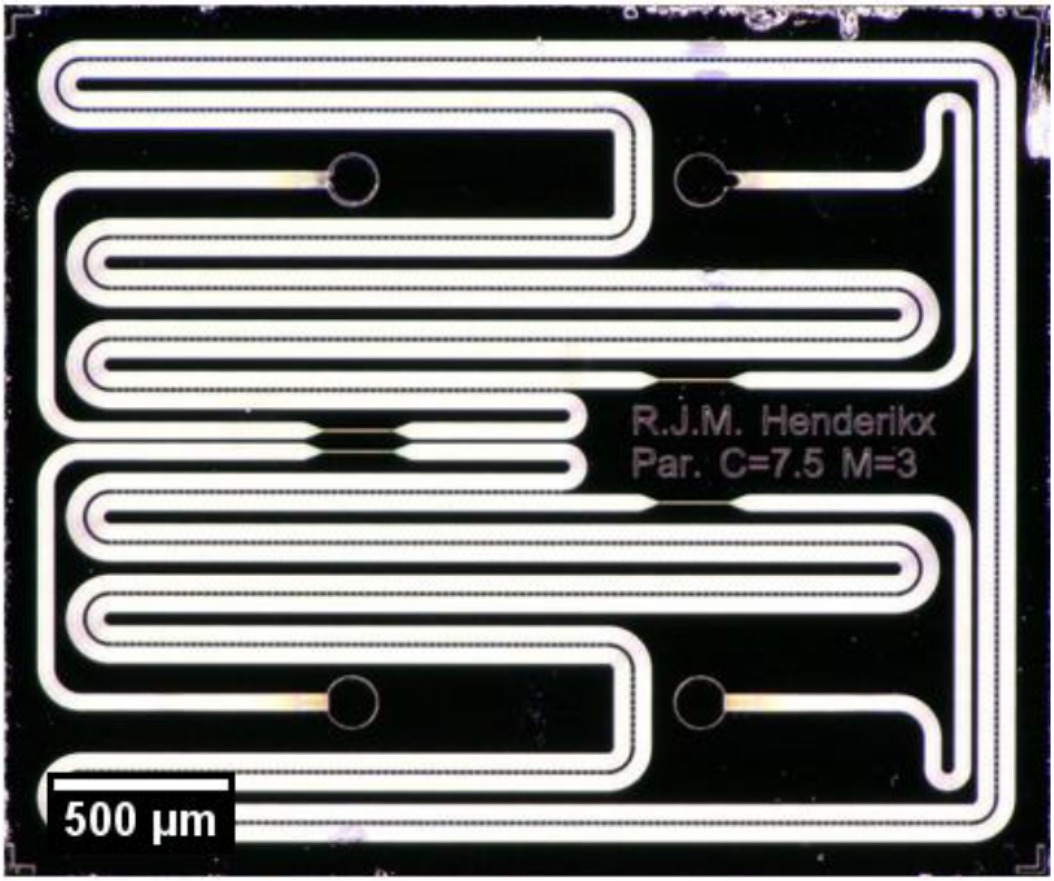

Figure 37: R.J.M. Henderikx's redesign. [23]

6 Conclusion

The use of microfluidics in medical studies, in particular medicine testing, prevents results that are an average of different outputs. Samples are more homogeneous and thus the results will be more reliable and specific to a certain type of sample. In medical microfluidics, several processes can be integrated on one chip, allowing for various experiments that normally need separate investigations to be performed at the same time. These are all advantages that make microfluidic devices an interesting subject in medical studies. However despite all these advantages, medical microfluidic devices are not a big commercial success. The main reason for this problem is the main material used to fabricate these devices. PDMS is not a mass-production friendly material and the fabrication method of PDMS based medical microfluidic devices is difficult and time consuming.

In this thesis a fabrication method for microfluidic devices was presented, where the main obstacle of silicon being opaque to visible light was solved. A microfluidic device was designed that used cell mechanobiology to test the effects of medicine on cells. This device that can be fabricated with purely Silicon microfabrication techniques, allows for many advantages including:

1- Possibility of using the vast existing IC manufacturing infrastructure for commercial manufacture.

2- Automated manufacturing.

3- Possibility of adding various CMOS sensors to the design of the device

A medical microfluidic device with such advantages is much more suitable for mass-production than the more common PDMS devices.

In relation to this research, R.J.M. Henderikx has redesigned a new device using the same method and investigated whether the effect of Cytochalasin-D on the mechanical properties of monocytes can be measured.

Bibliography

[1] G. M. Whitesides, "The origins and the future of microfluidics," *Nature,* vol. 442, pp. 368-373, 2006.

[2] G. T. Vladisavljević, N. Khalid, M. A. Neves, T. Kuroiwa, M. Nakajima, K. Uemura, *et al.*, "Industrial lab-on-a-chip: Design, applications and scale-up for drug discovery and delivery," *Advanced Drug Delivery Reviews,* vol. 65, pp. 1626-1663, 2013.

[3] C. Ahn and J.W. Choi, "Microfluidics and Their Applications to Lab-on-a-Chip," in *Springer Handbook of Nanotechnology*, B. Bhushan, Ed., ed: Springer Berlin Heidelberg, 2007, pp. 523-548.

[4] C. Holtze, "Large-scale droplet production in microfluidic devices - an industrial perspective *Journal of physics D: Applied physics,* Vol. 46(11), 2013

[5] H. Yin and D. Marshall, "Microfluidics for single cell analysis," *Current Opinion in Biotechnology,* vol. 23, pp. 110-119, 2012.

[6] L. R. Volpatti and A. K. Yetisen, "Commercialization of microfluidic devices," *Trends in Biotechnology,* vol. 32, pp. 347-350, 2014.

[7] R. v. d. Laar, Operation Manual Novellus, Philips Research and Innovation, 2010.

[8] "Flexus F-5200 stress meter," Nanolab foundation, [Online]. Available: http://www.nanolabnl.nl/facilities/database/239?view=tool. [Accessed 08 2015].

[9] P. N. Nge, C. I. Rogers, and A. T. Woolley, "Advances in Microfluidic Materials, Functions, Integration, and Applications," *Chemical Reviews,* vol. 113, pp. 2550-2583, 2013.

[10] E. W. K. Young, D. Beebe, "Engineers are from PDMS-land, biologists are from polystyrenia," *Lab on a Chip,* Vol. 12(11), pp. 1224–1237, 2012

[11] J. R. Lange, J. Steinwachs, T. Kolb, L. A. Lautscham, I. Harder, G. Whyte, *et al.*, "Microconstriction Arrays for High-Throughput Quantitative Measurements of Cell Mechanical Properties," *Biophysical Journal,* vol. 109, pp. 26-34, 2015.

[12] A. Ravetto, "Microfluidic devices for mechanical characterization and manipulation of monocytes," PhD Dissertation, Technische Universiteit Eindhoven, 2015

[13] D. Qin, Y. Xia, and G. M. Whitesides, "Soft lithography for micro- and nanoscale patterning," *Nat. Protocols,* vol. 5, pp. 491-502, 2010.

[14] Y. Kikuchi, K. Sato, H. Ohki, and T. Kaneko, "Optically accessible microchannels formed in a single-crystal silicon substrate for studies of blood rheology," *Microvascular Research,* vol. 44, pp. 226-240, 1992.

[15] I. Kobayashi, M. Nakajima, K. Chun, Y. Kikuchi, and H. Fujita, "Silicon array of elongated through-holes for monodisperse emulsion droplets," *AIChE Journal,* vol. 48, pp. 1639-1644, 2002.

[16] Y. Kikuchi, K. Sato, and Y. Mizuguchi, "Modified Cell-Flow Microchannels in a Single-Crystal Silicon Substrate and Flow Behavior of Blood Cells," *Microvascular Research,* vol. 47, pp. 126-139, 1994.

[17] N. Blow, "Microfluidics: the great divide," *Nature Methods,* Vol. 6(9), pp. 683-686, 2009

[18] E. Alexander, Operation Manual Cintillio Cleaning Tool, Philips Innovation and Services, 2011.

[19] Tencor Instruments, "Tencor Flexus 2320 Manual," 1994. [Online]. Available: https://snf.stanford.edu/SNF/equipment/characterization-testing/flexus-2320/Flexus2320.pdf/view. [Accessed 09 2015].

[20] C. E. Viana, A. N. da Silva and N. I. Morimoto, "Analysis of SiO2 Thin Films Deposited by PECVD Using an Oxygen-TEOS-Argon Mixture," Brazilian Journal of Physics, vol. 31, no. 2, pp. 299-303, 2 June 2001.

[21] G. S. Hwang, "On the origin of the notching effect during etching in uniform high density plasmas," Journal of Vacuum Science and Technology B: Microelectronics Processing and Phenomena, vol. 15, no. 1, p. 70, 1997.

[22] MicroChem, "Megaposit SPR660 Series Photoresist" 2014, [online], Available: http://www.microchem.com/PDFs_Dow/MEGAPOSIT_SPR_660.pdf. [Accessed 08 2015]

[23] R.J.M. Henderikx, " Microfluidic device to characterize the effect of chemical agents on mechanical properties of cells," Master Thesis, Eindhoven University of Technology, July 2016.

Acknowledgement

In this acknowledgement, I would like to thank many people who helped and guided me during both my internship and thesis project.

First, great gratitude to Prof. dr. Ronald Dekker, who supervised me during my internship and master project.

Second, thank you Ir. Ronald Stoute for your daily advices, guidance and help.

Third, I would like to also thank Marcus Louwers, Jaap Snijder, Eugene Timmering and everyone else at Philips Medical in Hightech Campus, Eindhoven, who helped me in various stages of my research.

Finally, I would like to offer my heartfelt thanks to my parents who have always supported my all through my life.

Appendix

Fabrication step	Tool	Process Details
5-1 Cleaning wafer	Cintillio cleaning tool	Remove contaminations from wafer surface.
5-2 SiO_2 Deposition	Novellus PECVD	SiO_2 PECVD deposition. 0.5µm at 400°C.
5-3 Lithography	EVG 150 wafer track	Photoresist: Pre-heat 150°C, Primer: HDMS, 800nm SPR660 (Dispense: 2000rpm, Spread: 3650rpm), BSR 1500rpm, Soft Bake 90s at 95°C
		Development: PEB 120°C, 40s in MF-26A at 21°C
	ASML stepper PAS5500/100	Exposure: Energy=240mj/cm^2 and Focus=-0.4µm for A designs. Energy=220mj/cm^2 and Focus=-0.4µm for B designs.
	Barrel IPC 9200	For 1 wafer: DESCUM O_2, 2-3min, 600W, Initial temp. 90°C
5-4 DRIE	STS CPX clustertool	SiO_2 etch: He, 10% CF_4 & 8% H_2, 3:30min Si DRIE: SF_6 & 10% O_2 (etch), C_4F_8 (passivation), 7min (B design) or 10min (A).
5-5 Si Isotropic Etch	Barrel Etcher IPC	Passivation layer removal: O_2 plasma, 10min, Initial temp. 90-100°C, 200W
		Si sidewall removal: CF_4 plasma, 10min, 50mTor, Initial temp. 130°C, 450W
5-6 Covering Trenches	Furnace LPCVD TEOS	Deposition of TEOS SiO_2, 1.5µm
Measurements	LOT Stress Measurement system	To Measure Bow and Stress of Wafers.
	Nanospect.	To Measure SiO_2 layer thickness after each Etching step.